ISSN 0869-5911, Petrology, 2015, Vol. 23, No. 1, pp. 45–67. © Pleiades Publishing, Ltd., 2015.
Original Russian Text © E.N. Kozlov, A.A. Arzamastsev, 2015, published in Petrologiya, 2015, Vol. 23, No. 1, pp. 50–74.

Petrogenesis of Metasomatic Rocks in the Fenitized Zones of the Ozernaya Varaka Alkaline Ultrabasic Complex, Kola Peninsula

E. N. Kozlov[a] and A. A. Arzamastsev[b]

[a]*Geological Institute, Kola Science Center, Russian Academy of Sciences, ul. Fersmana 14, Apatity, Murmansk oblast, 184209 Russia*
e-mail: kozlov_e.n@mail.ru

[b]*Institute of Precambrian Geology and Geochronology, Russian Academy of Sciences, nab. Makarova 2, St. Petersburg, 199034 Russia*
e-mail: arzamas@ipgg.ru

Received January 29, 2014; in final form, May 20, 2014

Abstract—This paper reports the results of an investigation of metasomatic alterations in basement gneisses within the contact aureole of the Ozernaya Varaka alkaline ultrabasic massif. Based on mineralogical and geochemical data, the metasomatic rocks were classified, variations in major and trace elements were evaluated along a cross-section through the contact zone, the mobility of components during the metasomatic transformation of rocks was estimated, and the gain or loss of components was quantified. The obtained results provided insight into the trends of changes in mineral assemblages, the mechanisms of migration of fluid flows, and, most importantly, the scale of input or removal of major and a number of trace components at different stages of the evolution of the metasomatic system within the contact aureole and border zones. It was shown that a fluid phase was released directly from a magma chamber filled with alkaline ultrabasic melt, which is indicated by the high $^3He/^4He$ value (5.9×10^{-6}) of the fluid, corresponding to 50% of the mantle component. It was shown that the release of a considerable amount of fluid phase related to the alkaline ultrabasic melt was not accompanied by a significant input of high field strength and rare earth elements. In contrast, the fluids of the subsequent carbonatite stage were enriched in volatile components (F, Cl, P, and S), which resulted in the migration of REE into the fenitized zones and removal of Ta, Zr, and Hf from it. The low $^3He/^4He$ value of this fluid suggests that its noble gases were contaminated by a crustal component, and solutions percolated along fracture systems and shatter zones from the root of the magmatic system. During the final postmagmatic stage, alkaline metasomatism was caused mainly by aqueous fluids and was accompanied by the removal of all rare earth elements and most of the high field strength elements (Nb, Ta, Zr, and Hf). A comparison of the fenitized zone of the Ozernaya Varaka complex with those of the Khibiny and Lovozero agpaitic syenite massifs showed that the metasomatic reworking of gneisses in the multiphase alkaline ultrabasic complex occurred in several stages and was accompanied by the input and removal of components, whereas the single-stage fenitization in the agpaitic syenite plutons involved minor amounts of heterogeneous water–fluoride fluids and resulted in extensive migration of rare earth and high-field strength elements in the contact zone.

DOI: 10.1134/S0869591115010026

INTRODUCTION

The investigation of the formation of metasomatic rocks in alkaline complexes is important in both fundamental and applied aspects. The emplacement and crystallization of alkaline and carbonatite magmas are accompanied by changes in their compositions owing to the migration of components and/or bimetasomatic exchange with the country rocks. The examination of the products of metasomatic alteration provides insight into the scale of mass transfer and important geochemical characteristics of migrating solutions and their evolution in time, which improves our understanding of the convergent development of alkaline intrusions and their host rocks. Furthermore, the contact zones of alkaline ultrabasic massifs are unique natural objects for the determination of conditions of fluid mobilization and transport of large ion lithophile elements (LILE), high field strength elements (HFSE), and rare earth elements (REE), which are characteristic of aluminosilicate and carbonatite magmas.

Various aspects of the formation of metasomatic rocks in alkaline complexes have been the subject of numerous studies over several decades (Sergeev, 1959; Kukharenko et al., 1965; Currie and Ferguson, 1971; Evdokimov, 1982; Rubie and Gunter, 1983; Kresten and Morogan, 1986; Andersen, 1989; Bardina and Popov, 1994; Morogan, 1994; Sindern and Kramm, 2000; Drüppel et al., 2005; Rass et al., 2006; Arza-

mastsev et al., 2011). The analysis of available publications showed that, despite the continued interest to such objects, there are still significant gaps in the understanding of the alkaline ultrabasic complexes of the Kola province, which is one of the world's largest alkaline provinces. Moreover, most of the detailed investigations focused on metasomatic zones related to the formation of considerable volumes of carbonatites: Alnö (Sweden), Fen (Norway), Callander Bay (Canada), Swartbooisdrif (Namibia), and others. The influence of carbonatite-derived solutions could significantly affect the initial composition of rocks in contact zones, which hampers correct estimation of the scale of major and trace element migration at early stages of the formation of such complexes. Based on these considerations, the rocks at the contact of the Ozernaya Varaka intrusion, which contains only minor amounts of ultramafics and carbonatites, were used as a reference object.

The goal of our study was to determine the character of metasomatic imprint in the Precambrian country rocks during various stages of the development of alkaline ultrabasic complexes, starting from the emplacement and cooling of foidolite magmas. In addition to the geological and petrographic examination of rocks in contact zones, a variety of problems were considered: (1) classification of metasomatites from the zones of contact interaction and estimation of their relative age relationships, (2) determination of mineralogical and geochemical indicators of the influence of metasomatic processes of different ages, (3) analysis of major and trace element variations in a cross-section through the contact zone, (4) estimation of the degree of mobility of components during the metasomatic alteration of rocks, and (5) quantification of the gain and loss of components. The obtained results allowed us to determine the trends of changes in mineral assemblages, establish the mechanisms of fluid flow migration, and, most importantly, estimate the scales of the gain and loss of major and a number of trace elements during various stages of the evolution of the metasomatic system in the contact and border zones.

GEOLOGIC STRUCTURE, PETROGRAPHY, AND COMPOSITION OF THE CONTACT ZONE

The Ozernaya Varaka massif is located at the junction of the Belomorian block and the Imandra–Varzuga belt of the Karelides (southern Kola Peninsula). The country rocks are the medium- and fine-grained biotite–oligoclase gneisses of the Belomorian complex, which contains minor amounts of biotite–amphibole gneisses and garnet–plagioclase amphibolites. The age of the biotite–oligoclase gneisses is 2723 ± 17 Ma (Rizvanova et al., 1994). The central part of the Ozernaya Varaka massif is made up of alkaline ultramafic rocks, mostly nepheline pyroxenites and melteigites (Fig. 1a). The rocks of the complex were formed at 376.1 ± 2.9 Ma (Kramm et al., 1993). They are surrounded by a wide ring of foidolites of the second intrusive phase (ijolite-dominated) accounting for more than 60% of the intrusion area at the present erosion level. The third intrusive phase includes cancrinite and cancrinite–nepheline syenites occurring as scarce veins 1–2 m thick cutting the pyroxenites and foidolites. The latest rocks of the massif are carbonatites (mainly, calcitic), which form vein and stocklike bodies. Their age was estimated as 369.6 ± 5.3 Ma (Kramm et al., 1993). The size of the intrusion is not large, and the area occupied by the contact metasomatic aureole (0.66 km^2) is comparable with the area of the intrusive units (0.8 km^2) (Kukharenko et al., 1965; Arzamastsev et al., 2009). The southern and western contact zones of the massif were observed in outcrops and exposed in trenches and surface strippings. The complete section of the contact was examined in two boreholes penetrating both the contact aureole and the border zone over 200 m. Geological and petrographic investigations suggested that the main volume of the metasomatic rocks surrounding the massif was formed during the foidolite stage. In addition, it was found that the metasomatites of this stage (fenitized gneisses and fenites after gneisses) associate in the contact aureole of the massif with a variety of later hydrothermal–metasomatic rock of varying age and diverse chemical composition, including at least three generations of compositionally distinctive carbonatites and carbonated silicate rocks forming bodies of diverse morphology. Note that this paper focuses only on the data for the carbonatites and carbonate–silicate rocks that occur in the contact aureole of the Ozernaya Varaka Massif and are hosted by fenites or fenitized gneisses. According to the classification of Samoilov (1984), these carbonatites and carbonate–silicate rocks correspond to the K-feldspar–calcite, albite–calcite, and chlorite–sericite–ankerite temperature facies. Several pieces of evidence for hydrothermal–metasomatic origin were found in the three identified types of rocks of the carbonatite stage: (1) metasomatic zoning of a certain type in the veins of carbonated silicate rocks of the K-feldspar–calcite temperature facies (from the vein axis): silicate–calcite carbonatite → basic rocks (mainly calcite–pyroxene) → alkaline metasomatites after fenite, and the volume of zones of the metasomatic column is proportional to the vein size; (2) the morphology of bodies of these rocks (thin veins, stringers, and schlieren "permeating" the host fenites); carbonatites of the albite–calcite facies form fracture-filling veins, with calcite euhedral against coexisting mafic minerals, which indicates their hydrothermal origin; and (3) the presence of shadow structures of early carbonatites related to the formation of complete carbonate pseudomorphs after mafic minerals in the rocks of the third type. This is consistent with the conclusion of Samoilov (1984) on the strong dominance of metaso-

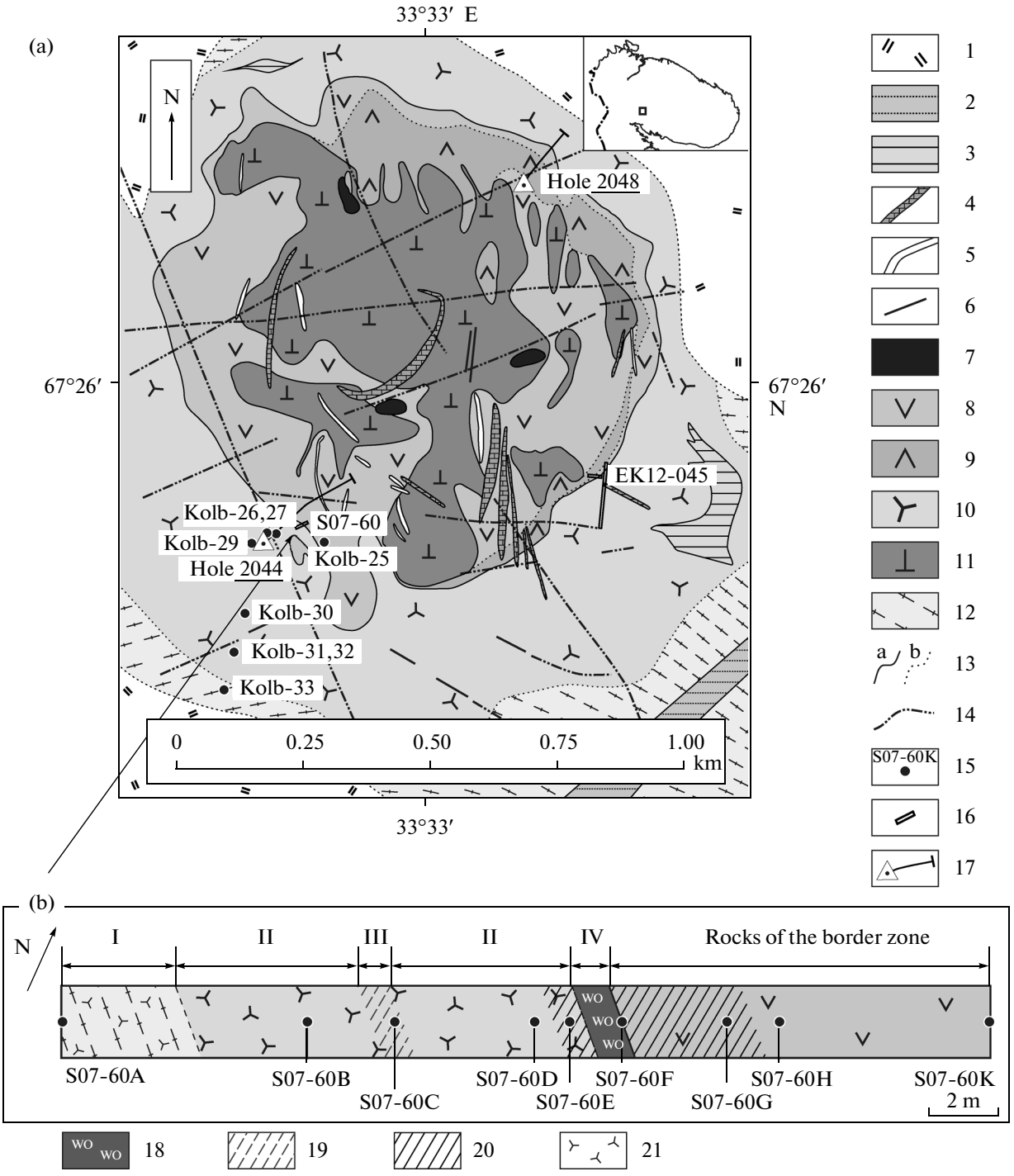

Fig. 1. (a) Schematic geologic structure of the Ozernaya Varaka complex according to the data of Murmansk Geological Expedition, Dudkin et al. (1980), and Arzamatsev et al. (2009) and (b) detailed cross-section through the contact in the southwestern part of the massif. The inset shows the position of the massif in the Kola Peninsula. (1) Quaternary deposits; (2) chalcedony breccia in shatter zones; (3) fenite breccia with an aegirine–albite cement; (4) carbonatite; (5) cancrinite–nepheline syenite; (6) dike complex: monchiquite, ijolite porphyry, and tinguaite; (7) alkaline pegmatoid; (8) ijolite; (9) melteigite; (10) fenite and fenitized gneiss; (11) pyroxenite; (12) biotite–oligoclase gneiss; (13) geologic boundaries, (a) sharp and (b) gradational; (14) fault; (15) sampling site; (16) area of detailed studies; (17) borehole top and projection on the surface; (18) wollastonite–clinopyroxene rock; types of metasomatic overprint are shown by fill patterns: (19) albitization; (20) high-temperature basic metasomatism; and (21) fenitization. Roman numerals indicate the boundaries of the occurrence of rocks of the distinguished zones. The UTM (WGS 84) coordinates of the contact at site S07-60 studied in detail were determined as X = 497 439 and Y = 7 479 437.

matic carbonatites over igneous ones in hypabyssal complexes, such as the Ozernaya Varaka Massif.

The investigation of textural relations allowed us to distinguish three groups of metasomatites corresponding to three stages of metasomatic alteration (in the order of their formation):

(1) synmagmatic alkaline metasomatites (fenitized gneisses and feldspar–clinopyroxene fenites after gneisses);

(2) hydrothermal–metasomatic rocks of the carbonatite stage, mostly basic in composition (carbonatites of the K-feldspar–calcite and albite–calcite temperature facies and a genetically related metasomatic complex, including wollastonite–clinopyroxene rocks); and

(3) postmagmatic hydrothermal–metasomatic rocks of mainly alkaline composition (phlogopite glimmerites, feldspar (albite and K-feldspar) metasomatic rocks, and aegirinites).

Although the metasomatites of the second and third groups are of minor significance in the structure of the contact aureole, metasomatites of different age are spatially closely associated in the sections examined, and most of the samples should therefore be considered as integrated products of several metasomatic processes. For our purposes, the southwestern cross-section of the contact zone appeared to be most representative; on the one hand, metasomatites of all the groups occur there, and, on the other hand, products of metasomatic alteration of different stages are not spatially superimposed. The cross-section displays the following sequence of metasomatic rocks (toward the contact) (Fig. 1b): fenitized gneisses (zone I), quartz-free clinopyroxene–feldspar fenites after gneisses (zone II) with areas of extensively albitized rocks (zone III), and wollastonite–clinopyroxene rocks (zone IV). Biotite–oligoclase granitic gneisses are protoliths for the rocks of all four zones.

Zone I is composed of quartz-bearing feldspar-dominated rocks containing 25–30% newly formed minerals. The metasomatic alteration of gneisses resulted in the formation of amphibole–pyroxene pseudomorphs after biotite and clinopyroxene rims around quartz grains and oligoclase replacement by an albite–K-feldspar aggregate. In terms of structure and texture, the fenitized gneisses are similar to the enclosing plagiogneisses; foliation and banding are clearly observed in these rocks. Primary metamorphic textures are associated with abundant corroded areas consisting entirely of newly formed phases (clinopyroxene, albite, K-feldspar, etc.) and showing a chain-like or streaky distribution in the rock.

In *zone II*, the transition from fenitized gneisses to clinopyroxene–feldspar fenites after gneisses is accompanied by the loss of the gneissic structure and development of coarse banding with alternating leucocratic (feldspar-dominated) and melanocratic (enriched in aegirine–augite) layers. In terms of mineral composition, the transition is marked by the disappearance of quartz, oligoclase, biotite, and alkali amphiboles; a change in clinopyroxene composition; and an increase in the content of K- and Na-feldspars.

The albitized areas (*zone III*) among the fenites after gneisses comprise leucocratic veins, stringers, and pockets consisting mainly of albite (75–80 vol %) and K-feldspar (15 vol %) with minor amounts of aegirine–augite (5–10 vol %). The thickness of veins and stringers ranges from a few millimeters to tens of centimeters. A characteristic feature of the rocks of albitized areas is significant depletion in apatite and titanite, which are typical accessory minerals of the fenites after gneisses.

The area of wollastonite–clinopyroxene rocks (*zone IV*) is 1.0–1.5 m thick and occurs directly at the contact of ijolites with fenitized country rocks. The boundary with ijolites is sharp and discordant. The wollastonite–clinopyroxene rocks show nonuniform structures consisting of an aegirine–augite matrix with numerous small (up to 2 cm thick) wollastonite veinlets, schlieren, and pockets, which contain up to 10 vol % apatite. The adjoining clinopyroxene–feldspar fenites occurring in the country rocks are cut by numerous thin stringers composed of wollastonite, clinopyroxene, calcite, apatite, and titanite.

The border zone of the intrusion observed in the cross-section is made up of heterogranular schorlomite ijolites and melteigites consisting of diopside (35–70 vol %), nepheline (20–50 vol %), and schorlomite (2–5 vol %). As the color index increases, the poikilitic nepheline crystals become less euhedral, and the size of clinopyroxene inclusions increases. Isometric schorlomite grains contain nepheline and clinopyroxene inclusions. Nepheline is replaced by veins and patches of cancrinite, and schorlomite is replaced by titanite. A thin (2.5–4.0 m thick) zone of massive fine-grained metasomatic rocks after ijolite was observed near the contact. It consists mainly of clinopyroxene (diopside) and is free of schorlomite. The mineral compositions of samples from this section and protolith rock (granitic gneiss) are given in Table 1. In addition, the mineral composition of sample 2048/263.3 of carbonated silicate rocks is listed in the table. The calcite + wollastonite + clinopyroxene (hedenbergite) + nepheline + garnet (andradite) assemblage indicates its assignment to the highest temperature portion of the K-feldspar–calcite temperature facies (750–1020°C) (Sokolov, 1996).

METHODS AND SAMPLES

In this study, we used samples from two detailed cross-sections (in the southwest and southeast of the massif, Fig. 1) and boreholes 2044 and 2048 penetrating the fenitization zone (overall, 120 samples). The contents of major elements were determined by

Table 1. Semiquantitative modal compositions (vol %) of rock samples from site S07-60 studied in detail in the southwestern part of the Ozernaya Varaka Massif, protolith (granite gneiss), and carbonated silicate rock of the K-feldspar–calcite temperature facies

Mineral phase	Protolith	*Zone I	Zone II	Zone III	Zone II	Zone II	Zone IV	Rocks of the border zone		Carbonatite
	Kolb-33	S07-60A	S07-60B	S07-60C	S07-60D	S07-60E	S07-60F	S07-60G	S07-60H	2048/263.3
Plagioclase	49.9	4.7	–	–	–	–	–	–	–	–
K-feldspar	9.4	15.2	17.4	16.1	20.2	16.9	0.8	–	–	–
Quartz	34.4	16.6	–	–	–	–	–	–	–	–
Biotite	4.7	0.1	–	–	–	–	–	–	–	–
Amphibole	–	0.3	–	–	–	–	–	–	–	–
Albite	–	56.9	65.6	77.5	63.3	61.6	5.9	–	–	–
Clinopyroxene	–	5.3	13.9	6.2	12.5	11.9	29.1	79.7	38.2	18.6
Wollastonite	–	–	–	–	–	0.4	48.4	0.5	–	22.0
Nepheline**	–	–	–	–	–	–	–	6.7	50.0	15.7
Garnet	–	–	–	–	–	–	–	–	4.0	6.4
Titanite	0.4	0.5	0.6	Tr.	0.2	0.3	0.3	2.1	2.5	2.7
Apatite	0.3	0.2	0.6	0.1	0.6	1.0	5.0	5.3	2.1	3.1
Calcite	0.3	–	1.7	Tr.	3.0	7.8	10.4	4.4	2.2	30.7
Sulfides***	0.2	0.2	0.2	0.1	0.2	Tr.	0.2	0.1	0.8	0.8
Fe hydroxides	0.5	Tr.	Tr.	Tr.	Tr.	Tr.	Tr.	1.1	0.2	Tr.

Sample S07-60G is metasomatic clinopyroxene rock after ijolite at the contact, sample S07-60H is schorlomite ijolite from the border zone of the intrusion, and sample 2048/263.3 is carbonatite of the K-feldspar–calcite temperature facies. * Here and in Tables 2, 4, 5, and 7, the assignment of the sample to the rocks of a particular zone is indicated (see text for explanation). ** The total content of nepheline and cancrinite replacing nepheline is given. *** Mainly, pyrrhotite and pyrite.

atomic absorption at the Geological Institute, Kola Science Center, Russian Academy of Sciences. Measurements were carried out using a single charge after rock decomposition by fusion with sodium tetraborate and sodium carbonate. The analytical precision was better that ±1.5% for contents >10% and ±3.5% for contents >1%. Minerals were identified using a LEO-1450 electron microscope with a RÖNTEC energy-dispersive detector. The compositions of minerals were determined on an MX-45 CAMECA electron microprobe with wavelength dispersive spectrometers at an accelerating voltage of 22 kV and a beam current of 30 nA. Natural and synthetic substances were used as standards. The analytical uncertainties were 1, 2.5, and 5% for contents of 10, 1, and 0.25 wt %, respectively. Trace elements were determined at the Open Analytical Center of the Tananaev Institute of Chemistry and Technology of Rare Elements and Mineral Raw Materials, Kola Science Center, Russian Academy of Sciences by inductively coupled plasma mass spectrometry (ICP-MS) using an ELAN 9000 DRC-e quadrupole spectrometer. Helium isotope ratios and contents were measured on a MI-1201 static mass spectrometer. The mass spectrometer resolution was sufficiently high (~1000) for the efficient separation of $^3He^+$ from the $^3He^+$–HD^+ doublet. The sensitivity for He was 5×10^{-5} A Torr^{-1}. The uncertainties of $^4He/^3He$ determination at 10^6 and 10^8 were 2 and 20%, respectively.

MINERALOGY OF CONTACT ZONES

The investigation of major (feldspars, pyroxenes, and wollastonite) and accessory minerals (apatite, titanite, and carbonates) allowed us to determine the sequence of mineral formation and distinguish several mineral assemblages in each of the aforementioned zones on the basis of the observed character of localization of the zones in the rocks and characteristic features of the composition and microtextural relations of mineral phases. Several assemblages were identified in most rock samples from these zones at variable quantitative relations of mineral phases of different age, which is related to the varying degree of metasomatic transformations and resistance of minerals to secondary processes. The compositions of assemblages and the chemistry of their minerals are given in Tables 2–4.

Quartz (Qz) grains in the fenitized gneisses are commonly surrounded by amphibole (far from the contact) and pyroxene (near the fenite zone) rims. In contrast to quartz from the unaltered gneisses, quartz from the fenitized gneisses does not show undulatory extinction. Small inclusions of newly formed clinopyroxene were occasionally observed in the marginal parts of quartz aggregates. Quartz disappears completely in zone II.

Plagioclase (Pl) is a typical mineral of gneisses and, similar to quartz, occurs as a relict phase in the zone of fenitized gneisses. The plagioclase of the gneisses is oligoclase in composition ($An_{27\text{-}31}$). A more sodic oligoclase variety, $Ab_{79}An_{19}Or_2$, was detected in the rocks

Table 2. Compositions of the mineral assemblages distinguished in the rocks of zones I–IV and carbonatites

Assemblage	Zone I	Zone II	Zone III	Zone IV	Carbonatites
Protolith	[*Qz*], [*Pl*], [*Mc*], [*Bt*]	–	–	–	–
Early alkaline	Ab_1, Kfs_1, [*Frct*], Ttn_1	Ab_1, Kfs_1, *Aeg-Aug*$_1$, [*Di*], Ap_1	Ab_1, Kfs_1, *Aeg-Aug*$_1$	*Aeg-Aug*$_1$, [Ap_1]	–
Basic	*Hd*	*Aeg-Aug*$_2$, [*Ano*], Ap_2(Sr), Ttn_2(Nb)	*Aeg-Aug*$_2$, [Ap_2(Sr)]	*Wo*, *Cal*, [*Ano*], Ap_2(Sr)	*Wo*, *Cal*, *Hd*, *Aeg-Aug*$_2$, *Nph*, *Ano*, *Grn**, Ap_2(Sr), Ttn_2(Nb)
Late alkaline	–	Ab_2, Kfs_2, Ap_3 (Sr, REE), Ttn_3(Sr)	Ab_2, Kfs_2, Ap_3(Sr, REE)	–	–

Mineral abbreviations: *Qz*, quartz; *Pl*, oligoclase; *Mc*, microcline; *Bt*, biotite; *Ab*, albite; *Kfs,* K-feldspar; *Ano*, anorthoclase; *Nph*, nepheline; *Frct*, ferrorichterite; *Hd*, hedenbergite; *Di*, diopside; *Aeg–Aug*, aegirine–augite; *Cal*, calcite; *Grn*, garnet; *Ttn*, titanite; and *Ap*, apatite. Minerals shown in brackets are relict phases, and distinctive compositional features are given in parentheses.
Garnet is assigned to this assemblage conditionally and is probably an autometasomatic phase.

of zone I. Plagioclase of such a composition occurs in the central parts of zoned feldspar grains and is clearly distinguished optically owing to extensive sericitization. From core to rim, oligoclase is replaced by monomineralic albite and further rimmed by albite–K-feldspar intergrowths. The newly formed phases are not affected by secondary alteration. Oligoclase disappears at the transition to zone II rocks.

Biotite (Bt) is the main mafic mineral of the unaltered gneisses. Biotite was also found in a few carbonatite samples. The composition of biotite corresponds to the annite–phlogopite solid solution series with equal fractions of the end-members (Bt_1; $X_{Ann} = 0.50$ and $X_{Flg} = 0.50$). Biotite resorption and replacement by amphibole were observed even far from the contact. Near the fenite zone, there are only rare poorly preserved biotite laths rimmed by albite–K-feldspar aggregates and/or replaced by amphibole and microgranoblastic clinopyroxene segregations. Similar to the other phases of the protolith assemblage, biotite completely disappears at the transition to the fenites after gneisses of zone II. The carbonatites contain subhedral biotite grains, the composition of which is similar to that of biotite from the gneisses (Bt_2, $X_{Ann} = 0.44$ and $X_{Flg} = 0.56$).

Amphibole (Frct) is a typical newly formed mineral in the fenitized gneiss zone. It was never observed in the unaltered gneisses. In the rocks of zone I, it forms homoaxial pseudomorphs after biotite and rims around quartz grains. In addition, fine acicular or fibrous amphibole aggregates fill fractures and voids in the rocks of this zone. Like biotite, amphibole becomes unstable toward zone II and is replaced by microgranoblastic clinopyroxene aggregates. The compositions of analyzed amphibole grains from zone I correspond to ferrorichterite following the IMA nomenclature (Leake et al., 1997).

Various *K- and Na-feldspars* occur as major minerals in the unaltered gneisses, as well as in the rocks of zones I, II, and III and in several carbonatite samples of the K-feldspar–calcite temperature facies. Microcline (*Mc*) is widespread in the gneisses, and its relict grains were documented in zone I rocks, where they underwent dissolution, pelitization, and recrystallization, up to the complete obliteration of polysynthetic twinning. In addition, fine-grained albite–K-feldspar aggregates (Ab_1 and Kfs_1) were observed in zone I; they replace relict oligoclase and form rims around resorbed biotite laths. Albite and K-feldspar are the most abundant minerals of zone II fenites. Their compositions are similar to those of Ab_1 and Kfs_1 from the fenitized rocks of zone I (correspondingly, $Ab_{99\text{-}96}An_{0\text{-}3}Or_1$ and $Or_{92\text{-}85}Ab_{7\text{-}15}An_{0\text{-}1}$, without Ba and Sr). The albite mole fraction of the K-feldspar tends to increase toward the contact. In addition, some fenite samples contain glomeroblastic aggregates of subhedral anorthoclase grains ($Ab_{75}Or_{24}An_1$; An_0) extensively replaced by K-feldspar and albite. Feldspars from zone III have unusual compositions: in addition to Ab_1 and Kfs_1, there are Sr-bearing albite ($Ab_{93}An_6Or_1$; Ab_2) and Ba–Sr-bearing K-feldspar ($Or_{87\text{-}89}Ab_{11\text{-}13}An_0$; Kfs_2). Microscopic inclusions of celsian ($BaAl_2Si_2O_8$) are ubiquitous in feldspar oikocrysts. The wollastonite–pyroxene rocks of zone IV contain only rare strongly resorbed grains of anorthoclase ($Ab_{51}Or_{48}An_1$) with elevated BaO contents (1.3 wt %). Similar compositional features were observed in alkali feldspars from the carbonatites of the K-feldspar–calcite temperature facies, in which anorthoclase ($Ab_{69}Or_{27}An_4$, 2.3 wt % BaO, and 1.9 wt % SrO) was also detected. However, the latter shows no reaction relations with other minerals of the carbonatite assemblage. Anhedral anorthoclase and calcite grains occur in these rocks in the interstices between subhedral clinopyroxene, apatite, and titanite grains and sometimes form poikilitic grains with inclusions of these minerals.

Among all the samples of metasomatic rocks from the contact aureole, *nepheline* (*Nph*) was found only in a few samples of carbonatites of the K-feldspar–calcite temperature facies, in which it associates with cal-

Table 3. Chemical compositions of minerals of the distinguished assemblages from the rocks of zones I–IV and carbonatites

Component	*Pl*	*Bt*	*Frct*	Ab_1	Ab_2	Kfs_1	Kfs_2	*Ano*	*Nph*	*Wo*	*Cal*	*Grn*	Ttn_1	Ttn_2	Ttn_3	Ap_1	Ap_2	Ap_3
SiO_2	63.30	37.14	52.43	68.76	67.33	65.42	64.43	68.06	43.37	50.89	0.15	34.24	30.11	30.57	30.72	0.31	0.33	1.24
TiO_2	–	2.48	0.13	–	–	–	–	–	–	–	–	5.93	35.07	33.41	38.00	–	–	–
Al_2O_3	22.99	11.99	0.53	19.23	20.33	17.59	17.75	18.32	31.04	–	–	2.69	0.52	1.30	0.20	0.05	0.00	0.07
FeO	0.22	20.23	–	0.45	0.00	0.22	0.06	0.23	0.32	0.63	0.00	22.42	1.69	2.09	1.33	–	–	–
MnO	–	0.06	0.30	–	–	–	–	–	–	0.27	0.12	0.31	0.05	0.00	0.00	–	–	–
MgO	–	11.54	8.45	–	–	–	–	–	–	0.11	0.00	0.34	–	–	–	–	–	–
CaO	3.93	0.00	7.13	0.06	1.22	0.21	0.00	0.17	0.84	47.82	54.83	33.35	27.42	27.98	27.40	56.16	53.99	51.78
Na_2O	8.92	0.25	4.44	11.71	10.36	1.00	1.39	8.26	16.04	–	0.00	–	0.56	0.00	0.46	0.10	0.11	0.22
K_2O	0.33	9.82	1.53	0.16	0.15	15.83	14.94	3.99	4.67	–	–	–	–	–	–	–	–	–
SrO	0.00	–	–	0.00	0.33	0.00	0.36	0.00	–	0.35	2.27	–	0.14	0.20	0.85	0.30	2.32	2.12
BaO	0.00	0.13	–	0.00	0.00	0.00	0.89	0.31	–	–	0.15	–	–	–	–	–	–	–
ZrO_2	–	–	0.00	–	–	–	–	–	–	–	–	0.25	1.07	0.28	0.00	–	–	–
Nb_2O_5	–	–	–	–	–	–	–	–	–	–	–	–	1.39	1.17	0.00	–	–	–
Ce_2O_3	–	–	–	–	–	–	–	–	–	–	0.18	–	0.28	0.65	0.00	0.11	0.44	1.46
P_2O_5	–	–	–	–	–	–	–	–	–	–	–	–	–	–	–	42.72	42.26	39.75
Total	99.56	93.64	97.79	100.37	99.72	100.27	99.74	99.33	96.28	100.06	57.71	99.53	98.30	97.65	98.96	99.75	99.45	96.64
*Atoms per formula unit																		
Si	2.81	2.92	7.99	3.00	2.96	3.02	3.00	3.03	1.08	2.97		2.81	1.00	1.00	1.00	0.05	0.06	0.21
Ti		0.15	0.01									0.37	0.88	0.82	0.93			
Al^{IV}	1.20	1.08	0.01	0.99	1.05	0.96	0.97	0.96	0.91									
Al^{VI}		0.03	0.09									0.26	0.02	0.05	0.01			
Fe^{3+}	0.00	0.00	0.00	0.02	0.00	0.01	0.00	0.01		0.03		1.37	0.05	0.06	0.04			
Fe^{2+}		1.33	2.91						0.01			0.21						
Mn		0.00	0.04							0.01		0.02	0.00	0.00	0.00			
Mg		1.35	1.92							0.01		0.04						
Ca	0.19	0.00	1.16	0.00	0.06	0.01	0.00	0.01	0.02	2.99	0.98	2.94	0.98	0.98	0.96	9.92	9.65	9.54
Na	0.77	0.04	1.31	0.99	0.88	0.09	0.13	0.71	0.77				0.04	0.00	0.03	0.03	0.04	0.07
K	0.02	0.98	0.30	0.01	0.01	0.93	0.89	0.23	0.15									
Sr	0.00			0.00	0.01	0.00	0.01	0.00		0.01	0.02		0.00	0.00	0.02	0.03	0.22	0.21
Ba	0.00	0.00		0.00	0.00	0.00	0.02	0.01										
Zr			0.00									0.01	0.02	0.00	0.00			
Nb													0.02	0.02	0.00			
REE***											0.00		0.01	0.01	0.00	0.01	0.04	0.20
P																5.96	5.97	5.79

Mineral abbreviations are given in Table 2 (see text for explanation).

* Mineral formulas were calculated on the basis of 8 O atoms for feldspars, 22 O for biotite, 23 O for amphibole, 4 O for nepheline, 6 O for wollastonite with separate calculation of Fe^{2+} and Fe^{3+}, 1 O for carbonates, 12 O for garnet with separate calculation of Fe^{2+} and Fe^{3+}, 1 Si for titanite, and 25 O for apatite. The formulas of mica and amphibole were calculated assuming that all iron is ferrous.

** Total content of rare earth elements.

Table 4. Chemical compositions of clinopyroxenes from the rocks of zones I–IV and carbonatites

Component		Zone I		Zone II		Zone III		Zone II				Zone IV		Carbonatites	
		S07-60A		S07-60B		S07-60C		S07-60E				S07-60F		2048/263.3	2044/153.6
		*C[a]	M[a]	C[e]	M[e]	C[e]	M[e]	C[e]	M[e]	C[a]	M[a]	C[e]	M[e]	C[e]	C[e]
SiO_2		50.85	50.48	51.47	51.67	52.69	51.35	52.36	52.99	54.56	52.73	51.66	51.62	50.40	51.28
TiO_2		0.10	0.03	0.37	0.29	0.13	0.29	0.10	0.15	0.05	0.16	0.18	0.20	0.36	1.13
Al_2O_3		0.78	0.57	1.66	0.75	0.31	0.46	0.35	0.67	0.74	0.70	0.69	0.91	1.56	1.99
FeO		17.62	20.48	17.46	21.21	12.69	18.64	14.71	16.95	5.08	17.85	13.67	14.07	16.19	15.62
MnO		0.36	0.45	0.50	0.78	0.31	0.93	0.58	0.96	0.20	1.05	0.42	0.36	0.47	0.40
MgO		6.94	4.89	5.98	4.31	9.37	5.95	7.93	5.69	14.34	5.98	8.13	7.71	7.82	7.02
CaO		20.91	20.37	14.72	13.19	19.94	15.97	19.50	17.41	23.09	16.80	19.03	20.42	21.59	16.13
Na_2O		1.47	1.74	5.96	6.19	2.97	4.82	3.63	4.04	1.34	4.70	3.57	2.66	1.81	4.78
Total		99.07	99.02	98.15	98.42	98.48	98.40	99.23	98.88	99.44	99.98	97.40	97.94	100.20	98.35
Distribution of cations among structural sites, calculated for 6 O and separating Fe^{2+} and Fe^{3+}**															
T	Si	1.98	2.00	1.96	1.99	2.00	1.98	1.99	2.04	2.01	2.00	1.99	2.00	1.93	1.95
	Al^{IV}	0.02	0.00	0.04	0.01	0.00	0.02	0.01	0.00	0.00	0.00	0.01	0.00	0.07	0.05
M1	Al^{VI}	0.02	0.02	0.04	0.03	0.01	0.00	0.00	0.03	0.03	0.03	0.02	0.04	0.00	0.04
	Fe^{3+}	0.10	0.12	0.43	0.43	0.19	0.37	0.27	0.18	0.05	0.31	0.24	0.15	0.19	0.29
	Ti	0.00	0.00	0.01	0.01	0.00	0.01	0.00	0.00	0.00	0.01	0.01	0.01	0.01	0.03
	Mg	0.40	0.29	0.34	0.25	0.53	0.34	0.45	0.32	0.79	0.34	0.47	0.45	0.45	0.40
	Fe^{2+}	0.47	0.56	0.13	0.25	0.22	0.24	0.20	0.37	0.11	0.26	0.20	0.30	0.32	0.21
	Mn	0.00	0.01	0.02	0.03	0.01	0.03	0.02	0.03	0.01	0.03	0.01	0.01	0.02	0.01
M2	Mg	0.00	0.00	0.00	0.00	0.00	0.00	0.00	0.00	0.00	0.00	0.00	0.00	0.00	0.00
	Mn	0.01	0.00	0.00	0.00	0.00	0.00	0.00	0.00	0.00	0.00	0.00	0.00	0.00	0.00
	Ca	0.87	0.86	0.60	0.55	0.81	0.66	0.79	0.72	0.91	0.68	0.79	0.85	0.88	0.66
	Na	0.11	0.13	0.44	0.46	0.22	0.36	0.27	0.30	0.10	0.35	0.27	0.20	0.13	0.35
***		*Hd*	*Hd*	*Aeg-Aug*$_2$	*Aeg-Aug*$_2$	*Aeg-Aug*$_1$	*Aeg-Aug*$_2$	*Aeg-Aug*$_1$	*Aeg-Aug*$_2$	*Di*	*Aeg-Aug*$_2$	*Aeg-Aug*$_1$	*Aeg-Aug*$_1$	*Hd*	*Aeg-Aug*$_2$

Oxides are given in wt %.

* Zone of analysis: C and M denote grain cores and margins, respectively; and indexes a and e indicate anhedral and euhedral grains, respectively.

** After Cawthorn and Collerson (1974).

*** Symbols of minerals are given in Table 2 (see text for explanation).

cite, hedenbergite, wollastonite, titanite, titanian andradite, and apatite. There are two morphological types of nepheline grains: anhedral segregations in the interstices between clinopyroxene, wollastonite, titanite, and apatite grains and isometric droplike inclusions in poikilitic calcite crystals. No reaction relationships were observed between calcite and nepheline. Nepheline grains are distinctly corroded at the boundary with garnet porphyroblasts. The composition of nepheline corresponds to the solid solution $Nph_{72}Kls_{14}Qz_{14}$.

Clinopyroxene is absent in the unaltered gneisses. On the other hand, it is a major mineral in the rocks of all the zones and carbonatites of the K-feldspar–calcite and albite–calcite temperature facies. Clinopyroxene grains show diverse morphology and chemical composition; their heterogeneity (zoning and patchy patterns) was distinguished by optical examination and back-scattered electron imaging. In the rocks of zone I, small (0.05–0.5 mm) anhedral clinopyroxene grains are assembled into segregations surrounding quartz grains and replace other mafic minerals (biotite and amphibole). According to the IMA nomenclature (Morimoto, 1989), the clinopyroxenes are assigned to the Quad chemical group and fall within the magnesian hedenbergite field (*Hd*, $Wo_{47}Fs_{31\text{-}16}En_{22\text{-}38}$). The rocks of zone II contain pyroxene grains of two morphological types: very small (0.05–0.3 mm) nonuniformly colored anhedral grains with embayed outlines often forming botryoidal aggregates and larger (0.2–0.5 mm and larger) optically uniform euhedral prismatic crystals forming trails in the rocks. The former type is irregularly distributed in the rocks and tends to occur in areas enriched in K-feldspar; and the latter type is confined to albite–carbonate veinlets. The cores of anhedral grains are also dominated by the Quad components and fall within the diopside field (*Di*, $Wo_{48\text{-}49}En_{38\text{-}42}Fs_{13\text{-}9}$). The central parts of euhedral crystals and margins of grains of both morphological types from zone II are Na–Ca pyroxenes classified as aegirine–augite, but their compositions are in most cases variable. Despite the high content of the aegirine end-member, the central parts of euhedral grains (*Aeg-Aug*$_1$, $Ae_{16\text{-}26}Jd_{4\text{-}1}$ $(Wo_{42\text{-}39}En_{22\text{-}23}Fs_{16\text{-}11})_{80\text{-}73}$) are chemically most similar to diopside from zone II (high Ca and Mg and low Mn). The margins of pyroxene grains from zone II (*Aeg-Aug*$_2$, $Ae_{26\text{-}44}Jd_{4\text{-}3}$ $(Wo_{35\text{-}26}En_{17\text{-}19}Fs_{19\text{-}7})_{70\text{-}53}$) show the highest contents of Na, Fe^{3+}, and Ti and the lowest contents of Ca and Mg. In addition, the rim zones are significantly enriched in MnO (up to 1 wt %). Clinopyroxene from the albitites of zone III underwent dissolution and replacement by K-feldspar and albite, and the compositions of grains correspond to *Aeg-Aug*$_1$ (central zones) and *Aeg-Aug*$_2$ (rim zones). All clinopyroxene grains analyzed in the wollastonite–clinopyroxene rocks of zone IV are chemically identical to *Aeg-Aug*$_1$ from zone II.

The compositions of pyroxenes from the carbonatites were also subdivided into two groups. The chemical composition of clinopyroxene from the highest temperature carbonated silicate rocks of the K-feldspar–calcite facies and surrounding basic metasomatites is similar to that from the fenitized gneisses of zone I and corresponds to magnesian hedenbergite ($Wo_{46\text{-}47}En_{33\text{-}27}Fs_{21\text{-}24}$). More alkaline pyroxenes occur in the lower temperature carbonatites of the albite–calcite facies; their compositions fall within the aegirine–augite field ($Ae_{27\text{-}31}Jd_{8\text{-}7}$ $(Wo_{34\text{-}31}En_{21\text{-}18}Fs_{10\text{-}12})_{66\text{-}62}$) and are similar to but slightly richer in the jadeite component than *Aeg-Aug*$_2$.

Wollastonite (Wo) is the major mineral of zone IV rocks and a few samples of K-feldspar–calcite temperature facies. The compositions of all the grains analyzed are fully consistent with the ideal stoichiometric formula $CaSiO_3$, and the content of additional components (FeO, MgO, MnO, and SrO) is no higher than 0.5 wt %.

Garnet (Grt) corresponding to titanian andradite in composition was found only in a few samples of carbonated silicate rocks of the K-feldspar–calcite temperature facies. Garnet porphyroblasts are isometric or anhedral up to 0.5 cm across with rough boundaries. Garnet often develops along fractures and margins of all mineral phases of this assemblage forming reaction rims or replacing them up to the appearance of complete pseudomorphs. This mineral was probably produced by the autometasomatic alteration of this rock type.

Carbonates occur in accessory amounts in most of the samples of zones I, II, and III and are major minerals in the wollastonite–pyroxene rocks, adjoining fenites, and all carbonatite varieties. Carbonates were observed mainly as anhedral grains in thin (a few millimeters thick) veinlets in association with albite, apatite, and late-generation clinopyroxene. In the wollastonite–clinopyroxene rocks, carbonate fills interstices between wollastonite and aegirine–augite grains. A similar textural position is characteristic of carbonate in the carbonated silicate rocks of the K-feldspar–calcite temperature facies. In fracture-filling veins of carbonatites of the albite–calcite temperature facies, carbonates are the most abundant minerals (up to 98 vol %), and their grains are euhedral against those of associating mafic silicates (clinopyroxene and biotite). The carbonates are dominated by calcite (*Cal*), which has identical chemical compositions in all samples, $Ca_{0.98}Sr_{0.02}(CO_3)$. In addition to calcite, diverse carbonates of Sr, Ba, REE, and Na are common, but their grains were too small for electron microprobe analysis.

Titanite is a typical accessory mineral of all the rocks studied and the main host for HFSE. The earliest generation of titanite (*Ttn*$_1$) was observed only in the fenites after gneisses of zone II; it shows elevated Na_2O contents (0.2–0.6 wt %) and is rich in Nb_2O_5 (up to 1.4 wt %) and ZrO_2 (up to 1.1 wt %). The second generation of titanite was observed in most of the car-

bonatite samples and occasionally in the fenitized gneisses and fenites of zones I and II. These titanites are also rich in Nb_2O_5 (up to 2.2 wt %) and ZrO_2 (up to 1.1 wt %), but their Na_2O content is no higher than 0.1 wt %. In the albitites of zone III, the early titanite generations are resorbed and leucoxenized, and rare newly formed titanite grains (Ttn_3) show elevated SrO (0.9 wt %) and Na_2O contents (0.4–0.5 wt %), whereas Nb, Ta, and Zr were not detected.

Apatite occurs in accessory amounts in the unaltered and fenitized gneisses, fenites, and albitized rocks. The content of apatite in the wollastonite–pyroxene rocks and carbonatites reaches 5 vol % and even more. Apatite occurs in the rocks of all zones as isometric or slightly elongated grains 0.3–0.5 mm in size without distinct crystal faces. The back-scattered electron images of apatite revealed pronounced internal heterogeneity in most grains. The results of apatite microanalysis are given in Table 3. In all the rock types studied, apatite is the main host for REE. With respect to trace element contents, three separate groups of apatite were distinguished: Ap_1 with low Sr and LREE contents, Ap_2 with high Sr and low LREE contents, and Ap_3 with high Sr and LREE contents. The analysis of the distribution of these apatite groups among different rock types and grain structures suggests their assignment to three generations. The earliest apatite (Ap_1) is confined to the cores of grains from the zone II fenites and wollastonite–clinopyroxene rocks of zone IV. Apatite of the second generation (Ap_2) forms rims on first-generation apatite grains and cores of apatite crystals in all the samples of carbonatites and albitized rocks from zone III. The latest apatite generation (Ap_3) was detected in the carbonatites and albitites of zone III, where apatite of the respective composition forms rims around second-generation apatite. The apatite generations have distinctly different mechanisms of REE incorporation in their structure. In particular, the isomorphic substitution $2Ca^{2+} \leftrightarrow REE^{3+} + Na^{+}$ prevails in Ap_1. The character of isomorphic substitutions changes continuously in Ap_2 toward the source of matter, up to the formation of Na-free varieties in the wollastonite–pyroxene rocks of zone IV and carbonatites. The composition of Ap_3 produced during albitization corresponds to the solid solution of apatite with the compositionally stable end-member $Ca_{1.4}Na_{0.75}REE_{2.85}(SiO_4)_{2.1}(PO_4)_{0.9}(OH,F)$. Compared with the apatite of the third generation from the albitites, carbonatite-hosted Ap_3 is strongly depleted in Na (0.00–0.02 a.p.f.u.), which indicates that the most important isomorphic substitution is $Ca^{2+} + P^{5+} \leftrightarrow REE^{3+} + Si^{4+}$.

GEOCHEMISTRY OF THE CONTACT ROCKS

The rocks of the contact aureole have widely variable major and trace element compositions (Tables 5, 6). The presence in the contact zone of geochemically distinctive metasomatites formed during different stages of the development of the multiphase massif does not allow us to distinguish systematic trends in the chemical composition of rocks toward the contact. On the other hand, there are a number of geochemical features which can be used in combination to discriminate between the rocks of different zones distinguished above.

Major elements. The granite gneisses and their partly metasomatized varieties (fenitized gneisses of zone I) show similar petrochemical characteristics, which is reflected in similar contents of most major oxides. The main characteristic feature of these rock types is the maximum silica content resulting in the presence of quartz. On the other hand, our investigations revealed systematic changes in the chemical composition of zone I rocks, including an increase in Na_2O and a decrease in SiO_2 toward the contact, i.e., with increasing degree of metasomatic alteration. Directly near the contact (in the fenites after gneisses of zone II), the SiO_2 content decreases, whereas the contents of most other major oxides, first of all, Na_2O, Al_2O_3, Fe_2O_3, and CaO, increase in a stepwise manner. The P_2O_5 content also increases considerably. The albitites of zone III show the maximum contents of Na_2O (8.99 wt %) and Al_2O_3 (15.58 wt %). The zone III rocks differ from the rocks of zone II with enclosing fenites in much lower contents of oxides of divalent cations, Fe_2O_3, TiO_2, and P_2O_5 and somewhat higher SiO_2 contents. The wollastonite–clinopyroxene rocks of zone IV and carbonatites show the most contrasting differences in major element characteristics from the other metasomatites of the contact zone of the Ozernaya Varaka Massif. Common feature of these rock groups are low (in the rocks of zone IV) and very low (in carbonatites) SiO_2 contents and lowest Al_2O_3, K_2O, and Na_2O contents accompanied by anomalously high CaO and P_2O_5. The rocks are also significantly enriched in F compared with the rocks of the protolith and zones I–III. In addition, the content of CO_2 is high in the wollastonite–clinopyroxene rocks and increases considerably further in the carbonatites.

The schorlomite ijolites from the border zone are almost indistinguishable from the ijolites of the interior of the massif in both major and trace element contents (Table 5). They are only slightly relatively depleted in SiO_2, Al_2O_3, MgO, and alkalis. However, it is noteworthy that the wollastonite–clinopyroxene rocks of zone IV are compositionally similar to the clinopyroxene metasomatites after ijolites occurring within the intrusion directly at the contact. These rock types are geochemically significantly different in the proportions of CaO, MgO, and FeO at total $R^{2+}O$ contents within 37–40 wt %.

Trace elements. The distribution of trace elements in the rocks of the contact zone of the massif is very irregular. The granite gneisses, which are protoliths for all the metasomatic rocks of the fenite aureole, show moderate contents of trace elements, no higher than

Table 5. Chemical compositions of rock samples from site S07-60 studied in detail in the southwestern part of the Ozernaya Varaka Massif, protolith (granite gneiss), and ijolite from the interior of the massif

Component	Protolith	Zone I	Zone II	Zone III	Zone II	Zone II	Zone IV	Rocks of the border zone		Ijolite
	Kolb-33	S07-60A	S07-60B	S07-60C	S07-60D	S07-60E	S07-60F	S07-60G	S07-60H	Kolb-25
SiO_2	71.49	69.70	60.23	63.43	61.77	56.29	43.81	45.42	40.81	42.28
TiO_2	0.36	0.21	0.30	b.d.l.	0.09	0.14	0.13	0.83	2.42	2.01
Al_2O_3	14.07	14.64	15.58	18.11	15.21	14.5	1.06	1.75	14.61	15.96
Fe_2O_3	1.47	0.57	2.07	0.46	1.27	1.34	2.38	6.01	5.37	9.86
FeO	1.07	1.24	1.64	0.67	1.35	1.61	2.93	7.86	4.73	b.d.l.
MnO	0.06	0.03	0.11	0.03	0.12	0.13	0.37	0.44	0.25	0.22
MgO	0.72	0.44	1.22	0.38	0.74	1.03	2.54	7.04	2.93	3.48
CaO	2.42	2.23	4.77	1.82	4.65	8.12	34.42	21.82	14.21	13.37
Na_2O	4.51	6.23	7.86	8.99	7.51	7.12	1.08	2.43	7.73	8.43
K_2O	2.07	2.35	2.72	2.58	3.07	2.6	0.1	0.05	2.14	2.38
P_2O_5	0.13	0.08	0.28	0.07	0.28	0.48	2.13	2.12	0.93	1.18
CO_2	0.11	b.d.l.	0.71	b.d.l.	1.26	3.31	3.71	1.48	0.83	0.56
S	0.11	0.09	0.10	0.06	0.11	0.02	0.07	0.05	0.38	0.03
Cl	0.010	0.009	0.009	0.009	0.011	0.008	0.019	n.a.	0.015	0.02
F	0.060	0.037	0.029	0.008	0.029	0.037	0.16	0.17	0.099	0.1
H_2O^+	0.86	1.59	1.46	2.59	1.7	2.12	3.77	2.09	1.36	0.56
H_2O^-	0.10	0.62	0.49	0.68	0.57	0.76	1.51	0.72	0.77	0.16
Total	99.62	100.07	99.58	99.89	99.74	99.62	100.19	100.28	99.58	100.60
Ba	626	787	1480	1052	1016	1277	87.2	181	53.1	41.2
Sr	291	557	1304	657	1251	2453	1554	1174	558	711
Li	16.4	8.81	4.36	1.06	1.42	1.36	2.08	5.03	5.99	2.78
Rb	7.42	53.1	25.8	18.9	24.2	17.0	1.26	1.77	33.5	32.0
Cs	0.85	0.25	0.11	0.15	0.01	0.05	0.16	0.13	0.30	0.18
Zr	26.9	60.1	135.3	20.5	19.5	58.5	71.8	92.1	389	377
Hf	1.04	1.79	2.81	0.66	0.61	1.07	1.40	2.54	8.94	9.05
Nb	17.2	63.6	104	28.5	19.8	24.5	143	40.5	89.6	165
Ta	0.95	6.92	7.98	8.72	3.96	3.68	3.55	2.15	6.67	10.8
Y	7.26	4.26	5.44	1.59	6.38	9.34	25.5	14.2	63.2	47.6
Sc	b.d.l.	44.1	11.0	20.2	5.77	5.46	8.05	17.6	3.50	4.45
La	27.9	27.5	46.4	22.9	89.8	134	190	148	66.2	81.4
Ce	49.5	59.1	90.1	34.3	143	232	316	260	135	175
Pr	5.31	5.80	10.00	3.13	13.8	23.7	30.0	27.4	17.3	21.3
Nd	17.7	16.9	29.2	8.67	37.6	84.7	79.4	81.6	64.3	83.7
Sm	2.99	3.03	5.56	1.41	5.77	12.9	14.0	15.0	16.9	16.7
Eu	0.99	0.84	1.58	0.50	1.45	2.48	3.65	2.48	5.50	5.19
Gd	2.37	2.68	4.70	1.20	5.10	9.68	14.1	11.1	18.0	14.4
Tb	0.34	0.21	0.39	0.09	0.37	0.79	1.16	0.86	2.37	2.18
Dy	1.45	0.96	1.69	0.36	1.76	3.16	6.14	3.57	13.9	11.6
Ho	0.28	0.17	0.28	0.06	0.28	0.47	1.04	0.57	2.64	2.05
Er	0.61	0.39	0.77	0.18	0.74	1.25	2.76	1.49	6.99	5.00
Tm	0.08	0.04	0.09	0.03	0.10	0.15	0.35	0.19	0.86	0.69
Yb	0.53	0.24	0.66	0.15	0.63	0.95	2.21	1.17	4.74	3.86
Lu	0.08	0.03	0.09	0.02	0.09	0.14	0.35	0.17	0.70	0.54
L*, m	245	16	9	6.5	2.5	1.5	0	–3	–4.5	–

Contents of oxides are in wt %, and elements are in ppm; n.a. means not analyzed, and b.d.l. is below the detection limit.

* Distance from the contact. The UTM (WGS 84) coordinates of the contact at site S07-60 were determined as $X = 497\,439$ and $Y = 7\,479\,437$.

Table 6. Chemical compositions of samples of carbonatites and carbonated silicate rocks from the fenite aureole of the Ozernaya Varaka Massif

Component	1*	1	2	2	3
	2048/263.3	2048/230.4	EK12-045L2	EK12-045P2	2048/232.6
SiO_2	28.56	25.74	6.25	2.06	38.3
TiO_2	1.84	1.49	b.d.l.	b.d.l.	0.68
Al_2O_3	7.01	1.6	1.59	0.4	9.07
Fe_2O_3	3.12	2.89	0.22	0.35	1.49
FeO	3.22	5.82	0.59	0.35	12.84
MnO	0.16	0.24	0.16	0.19	0.38
MgO	1.65	4.38	0.34	0.3	4.31
CaO	35.62	37.7	48.87	52.37	9.22
Na_2O	2.91	1.01	0.82	0.24	0.15
K_2O	0.59	0.06	0.24	0.08	0.94
P_2O_5	1.42	1.79	0.32	0.04	0.68
CO_2	12.06	15.74	35.95	39.91	17.86
S	0.67	0.22	b.d.l.	b.d.l.	0.53
Cl	0.016	0.007	0.02	0.012	0.014
F	0.14	0.17	0.088	0.065	0.12
H_2O^+	0.54	0.87	2.89	1.57	2.32
H_2O^-	0.16	0.18	0.14	0.14	0.7
Total	99.69	99.91	98.49	98.08	99.60
Ba	672	750	557	582	60.5
Sr	13300	11200	11600	12200	1610
Li	4.26	6.41	1.60	1.42	36.0
Rb	11.4	1.02	2.41	1.23	36.8
Cs	0.22	0.07	0.06	0.07	0.57
Zr	178	144	36.5	16.3	181
Hf	4.63	3.96	0.87	0.91	2.98
Nb	400	256	31.9	33.2	76.3
Ta	80.9	26.7	8.33	3.03	3.73
Y	32.24	32.8	49.0	53.8	22.4
Sc	6.95	10.34	2.36	2.42	6.67
La	552.60	776.11	385.62	399.24	159.24
Ce	803.60	1151.66	693.00	713.10	256.01
Pr	75.05	100.94	68.98	71.56	24.45
Nd	215.25	278.79	214.80	223.55	76.10
Sm	24.04	28.62	26.88	26.93	9.35
Eu	6.70	7.58	7.77	7.67	2.79
Gd	27.82	36.03	30.86	31.86	10.77
Tb	2.44	2.98	3.01	3.28	1.11
Dy	8.27	9.77	12.58	12.69	4.52
Ho	1.08	1.46	1.91	1.86	0.74
Er	2.93	3.64	4.86	4.93	2.00
Tm	0.36	0.45	0.72	0.69	0.28
Yb	2.05	2.59	4.33	3.91	1.94
Lu	0.20	0.42	0.78	0.51	0.34

Oxides are given in wt %, and elements, in ppm. b.d.l. indicates below the detection limit.

* Temperature facies of carbonatites after Samoilov (1984): (1) K-feldspar–calcite; (2) albite–calcite; and (3) chlorite–sericite–ankerite.

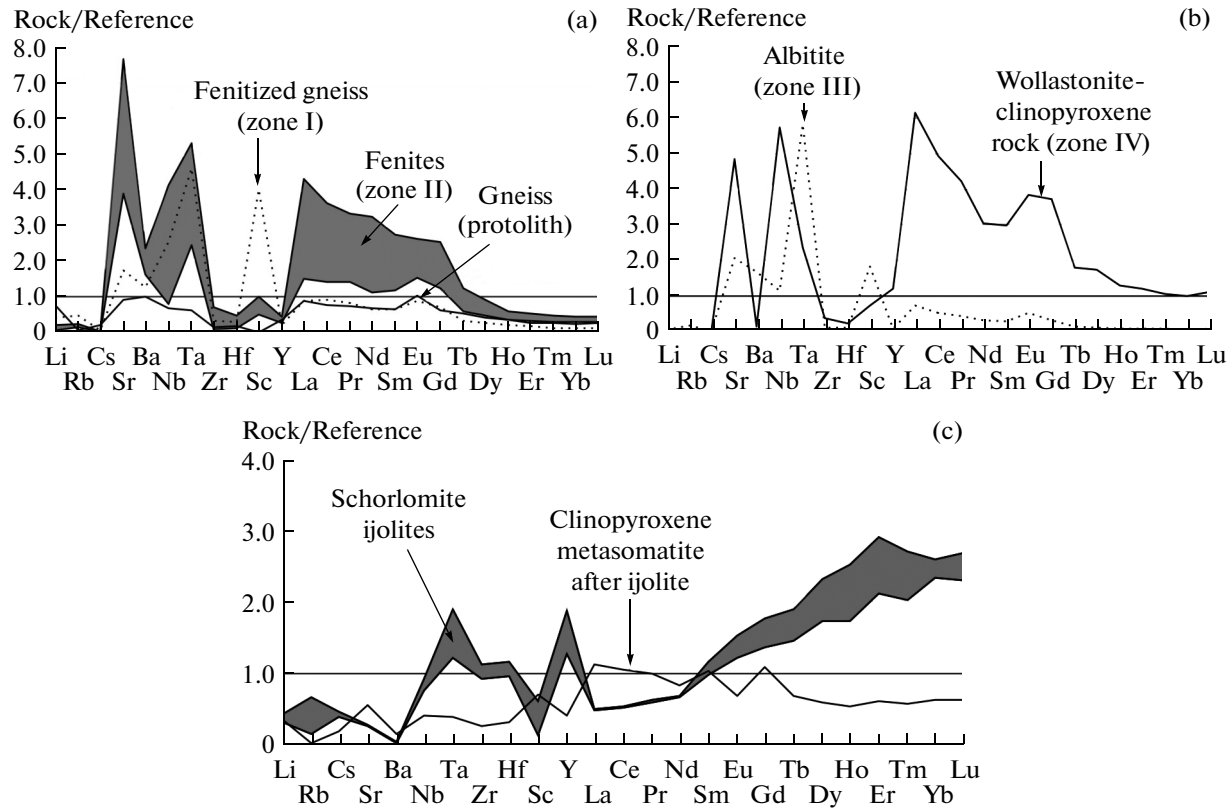

Fig. 2. Normalized trace element patterns of the (a) protolith (granite gneiss) and rocks of zones I and II; (b) rocks of zones III and IV; and (c) rocks from the border zone of the Ozernaya Varaka Massif. The following compositions were used for normalization: (a and b) median values of trace element contents in the upper crust (Taylor and McLennan, 1995; Wedepohl, 1995; Rudnick and Gao, 2003) for the protolith and rocks of zones I–IV and (c) weighted mean composition of the alkaline ultrabasic series of the Kola Province (Arzamastsev et al., 2001).

their upper crustal abundances (Fig. 2a). A comparison of the fenitized gneisses of zone I with the unaltered gneisses revealed similar contents of Zr, Hf, and REE and enrichment in Sr, Ba, Nb, Ta, and Sc. The transition to the zone II fenites is marked by an increase in Sr, Ba, and LREE contents. The process resulting in the formation of the zone III rocks caused significant REE loss and Sc gain (Fig. 2b). On the other hand, the wollastonite–pyroxene rocks of zone IV are enriched in the whole range of REE, the total content of which reaches a maximum of 687 ppm among all the analyzed silicate rocks from the contact zone of the massif. Another remarkable feature of these rocks is low Ba contents. Noteworthy is the contrasting distribution of Ta and Nb between the rocks of zones III and IV. The zone III albitites display a Ta peak at moderate Nb contents, whereas the zone IV rocks show the opposite relationship. This feature is reflected in Ta/Nb variations in the rocks of the section from the highest value in the albitites (0.31) to the lowest in the wollastonite–clinopyroxene rocks (0.02).

For the analysis of trace element distribution in the rocks of the border zone of the massif, the weighted mean composition of the alkaline ultrabasic series of the Kola Province was used as a reference for comparison (Arzamastsev et al., 2001) (Fig. 2c). A characteristic feature of the schorlomite ijolites is their enrichment in HFSE and HREE at moderately low LILE and LREE (La–Nd) contents. The contact clinopyroxene metasomatites after ijolites are depleted in almost all trace elements, except for LREE, the contents of which are similar to those in the weighted mean composition of the alkaline ultrabasic series.

The trace element contents of the carbonatites are different between different temperature facies and from the similar rocks of the contact zone (Table 6). Specific features of the carbonatites of the K-feldspar–calcite and albite–calcite facies are anomalously high contents of Sr (1.0–1.3 wt %) and REE (1500–2400 ppm). The carbonatites of the chlorite–sericite–ankerite temperature facies also show elevated contents of these elements approaching those observed in the wollastonite–clinopyroxene rocks of zone IV. The latter are similar to the carbonatites of the chlorite–sericite–ankerite facies in low Ba contents. The calcite carbonatites show varying HFSE contents: the highest values among all the rocks of the contact zone were observed in the carbonatites of the K-feldspar–calcite facies, and those of other carbonatite facies are an order of magnitude lower. Another distinctive parameter is the LREE/HREE ratio,

which is 19.9–23.9 in the carbonatites of the K-feldspar–calcite facies and 11.8–12.0 in the rocks of the albite–calcite facies.

The chondrite-normalized REE patterns of the rocks of the southwestern site studied in detail are shown in Fig. 3. For comparison, also shown are the REE patterns of the host granite gneisses (Fig. 3a) and ijolites from the interior of the massif (Fig. 3b). The REE patterns of the rocks of the contact zone and the schorlomite ijolites of the intrusion are significantly different. In particular, the ijolites have the least fractionated REE patterns compared with other rocks from the southwestern contact of the massif (Fig. 3b). They show gently sloping chondrite-normalized REE patterns without Eu and Ce anomalies, Eu/Eu* = 0.95–0.96, Ce/Ce* = 0.94, and $(La/Yb)_N = 9.4–10.3$. The REE patterns of the enclosing rocks are steeper and vary from zone to zone. The unaltered granite gneisses show minor Eu and Ce anomalies, Eu/Eu* = 0.90 and Ce/Ce* = 1.10, and the lowest $(La/Yb)_N$ value (37.4) among the rocks of the contact zone. The zone I rocks are similar to the gneisses in LREE contents but depleted in HREE, which results in an increase in $(La/Yb)_N$ up to 81.1. The REE patterns of the zone II fenites exhibit a weak Ce anomaly (Ce/Ce* = 0.87–0.95) and variable Eu/Eu* = 0.66–0.93 and $(La/Yb)_N = 49.6–101.0$. A characteristic feature of rocks from this zone is relatively low Y/Ho ratios ranging from 19.4 to 22.7. In other rocks of the contact aureole, this ratio is within 24.4–25.9 reaching 30.4 in the carbonatites. The zone III albitites have the lowest total REE contents of 75 ppm, and their REE patterns show a positive Eu anomaly (Eu/Eu* = 1.15), a negative Ce anomaly (Ce/Ce* = 0.84), and the maximum $(La/Yb)_N$ value (105.5) among all the silicate rock samples analyzed by us. The chondrite-normalized REE patterns of the wollastonite–clinopyroxene rocks are not distinctive. The rocks of zone IV are similar in most parameters (Eu/Eu* = 0.78, Ce/Ce* = 0.90, and $(La/Yb)_N = 60.7$) to the zone II fenites, except for higher Y/Ho values reaching 24.4 in the wollastonite–clinopyroxene rocks. An interesting observation is the similarity of contents and almost perfect coincidence of REE patterns in the clinopyroxene metasomatites after ijolite directly near the contact (sample S07-60G) and in the fenites adjoining the wollastonite–clinopyroxene rocks (sample S07-60E) (Fig. 3b). The REE patterns of all carbonatite varieties are similar in the LREE range (Fig. 3c) and show persistent minor negative Ce and Eu anomalies (Cr/Ce* = 0.82–0.93 and Eu/Eu* = 0.73–0.86). However, the difference in the proportions of LREE and HREE in the carbonatites of different temperature facies is clearly manifested in $(La/Yb)_N$ variations from 62.6–71.8 in the carbonatites of the K-feldspar–calcite facies to 189.6–210.8 in the carbonatites of the albite–calcite facies.

Quantification of the Gain and Loss of Components

A direct comparison of component contents is inappropriate for the estimation of mass transfer related to metasomatic processes, because the result is affected by density and porosity changes during metasomatic transformations, which may result in significant overestimation or underestimation of the gain or loss of components. Changes in the masses of major and trace components were estimated using a method based on the proportions of volumes and component contents between the protolith and altered rock (Gresens, 1967) simplified by Grant (1986). The change in the mass of a protolith component (ΔM_i) is described by the equation

$$\Delta M_i = [(M^A/M^O)C_i^A - C_i^O]M^O, \quad (1)$$

where M and C_i are the masses and contents of the component in the protolith (O) and altered rock (A), respectively. Changes in component content are described by the equation

$$C_i^O = M^O/M^A(C_i^O + \Delta C_i), \quad (2)$$

which is transformed for inert components to

$$C_i^A = (M^O/M^A)C_i^O. \quad (3)$$

In the C^O–C^A diagram, the contents of inert components will plot on the line of zero mobility with a slope of M^O/M^A passing through the origin ($C^O = 0$ and $C^A = 0$). Such a line is called an isocon (Gary et al., 1974). We used the isocon diagram method implemented in a computer program by Coelho (2006). The program allows estimating the gain and loss of components relative to the lines of constant mass, $C^A = C^O$, slope = 1, and volume, $C^A = (\rho^A/\rho^O)C^O)$, where ρ is the density of the protolith (O) and altered rock (A), respectively.

Using Eq. (1) and the calculated M^O/M^A ratio for any component, the absolute gain–loss values ($\Delta M_i/M^O$) and changes in the mass of the component relative to its mass in the protolith ($\Delta M_i/M_i^O$) can be estimated:

$$\Delta M_i/M^O = (M^A/M^O)C_i^A - C_i^O, \quad (4)$$

$$\Delta M_i/M_i^O = (M^A/M^O)C_i^A/C_i^O - 1. \quad (5)$$

Fig. 3. Chondrite-normalized REE distribution patterns of the rocks of (a) the contact aureole, (b) border zone of the intrusion, and (c) carbonatites of the Ozernaya Varaka Massif. For comparison, panel (b) shows the composition of fenite adjoining the wollastonite–clinopyroxene rock and ijolite from the inner part of the massif. The chondrite composition is after Anders and Grevesse (1989).

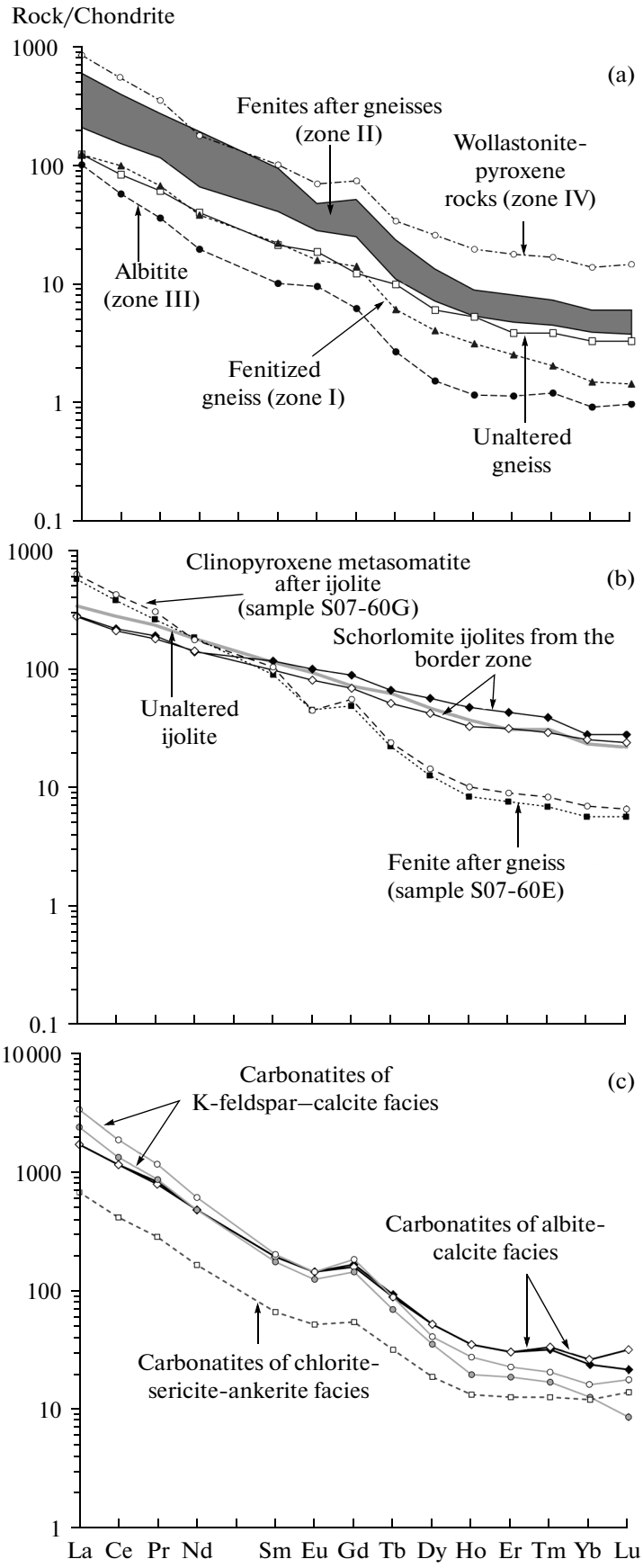
Rock/Chondrite
1000
100
10
1
0.1
(a)
Fenites after gneisses
(zone II)
Wollastonite-
pyroxene
rocks (zone IV)
Albitite
(zone III)
Fenitized
gneiss (zone I)
Unaltered
gneiss
(b)
Clinopyroxene metasomatite
after ijolite
(sample S07-60G)
Schorlomite ijolites from the
border zone
Unaltered
ijolite
Fenite after gneiss
(sample S07-60E)
10000
1000
100
10
1
0.1
(c)
Carbonatites of
K-feldspar–calcite facies
Carbonatites of albite-
calcite facies
Carbonatites of chlorite-
sericite-ankerite facies
La Ce Pr Nd Sm Eu Gd Tb Dy Ho Er Tm Yb Lu

Table 7. Calculation of the number of atoms of major components in a reference volume of 1000 Å on the basis of the atomic-volume system, chemical analyses of samples, and their submodal compositions (Kazitsyn and Rudnik, 1968)

Component	Zone I	Zone II	Zone IV	Carbonatite*	Zone III
	S07-60A	S07-60B	S07-60F	2048/263.3	S07-60C
Si	19.20	16.77	14.62	8.69	17.21
Ti	0.04	0.06	0.03	0.42	0.00
Al	4.75	5.11	0.42	2.51	5.79
Fe	0.40	0.82	1.42	1.53	0.25
Mn	0.01	0.03	0.13	0.04	0.01
Mg	0.18	0.51	1.26	0.75	0.15
Ca	0.66	1.42	12.31	11.61	0.53
Na	3.33	4.24	0.70	1.72	4.73
K	0.83	0.97	0.04	0.23	0.89
P	0.02	0.07	0.60	0.37	0.02
$C(CO_2)$	0.00	0.27	1.69	5.01	0.00
S	0.05	0.05	0.04	0.38	0.03
Cl	0.00	0.00	0.01	0.01	0.00
F	0.03	0.03	0.17	0.13	0.01
H(OH)	2.92	2.71	8.39	1.10	4.69
O	48.94	48.37	48.53	48.19	47.92

* Carbonated silicate rock containing approximately 30 vol % calcite.

The relative mobility of components during metasomatic processes is more adequately characterized by the $\Delta M_i / M_i^O$ parameter. In order to facilitate calculations, M^O is usually taken as 100 g. The correct application of this algorithm requires the solution of two key problems: (1) choice of a pair of protolith–altered rock samples for comparison and (2) estimation of the degree of element mobility and distinguishing inert components. For the simulation of mass transfer during various stages of the evolution of the metasomatic system, we used the compositions of the following pairs as initial materials: fenitized gneiss–fenite, fenite–wollastonite–clinopyroxene rock, fenite–metasomatic carbonatite of the K-feldspar–calcite temperature facies, and fenite–albitite. The choice of these pairs was based on a number of indicators of their assignment to a particular type of metasomatic materials (structural position in the section, presence of more than 90 vol % of cogenetic minerals in the sample, distinct manifestation of petrochemical characteristics, etc.). To solve the second problem (estimation of the degree of mobility), the numbers of atoms of major components in a reference volume of 1000 Å were determined for the selected samples. Calculations were carried out for an atomic-volume system on the basis of the chemical analyses and submodal compositions of the samples (Kazitsyn and Rudnik, 1968). The results are given in Table 7. The analysis of the obtained data showed that a transition from the fenitized gneisses to the clinopyroxene–feldspar fenites is accompanied by the accumulation of Na and divalent bases and minor desilication. Aluminum and K can be considered as weakly mobile elements. The wollastonite–clinopyroxene rocks and carbonatites are characterized by almost complete removal of alkalis and Al, significant removal of SiO_2, and extensive accumulation of bases (primarily, Ca). Since the wollastonite–clinopyroxene rocks and carbonatites were formed at a perfectly mobile behavior of all components, mass balance was calculated assuming constant volume during metasomatism. In the albitization zone, the relative contents of Na and Al increased, SiO_2 and K were weakly mobile, and divalent bases were removed.

The results of the isocon analysis of gain and loss revealed significant differences in the redistribution of trace components between the selected pairs of samples (Table 8). The model of fenitized gneiss transformation to fenite involves the relative accumulation of almost all REE and HFSE (Fig. 4a), although the absolute magnitude of element input is not high. Two groups of LILE can be distinguished: Ba and Sr were accumulated in the fenites, whereas Li, Cs, and Rb were transported into the country rocks. The behavior of volatiles was not uniform. The fenites were enriched relative to the fenitized gneisses in P and CO_2 but depleted in halogens. The evaluation of mass transfer during the formation of basic metasomatites (wollastonite–clinopyroxene rocks and carbonatites of the K-feldspar–calcite temperature facies) after apogneissic fenites (Figs. 4b, 4c) revealed some common features. In both cases, depletion in Ba and Cs was accompanied by enrichment in Sr, Rb, all REE, and Y, but the scales of Sr and REE input were different. The formation of wollastonite–pyroxene rocks associated with the uniform accumulation of both Ce and Y

Table 8. Calculation of the gain and loss of components for the rocks of the contact zone on the basis of isocon analysis (Coelho, 2006)

Component	S07-60A* / S07-60B**		S07-60B / S07-60F		S07-60B / 2048/263.3		S07-60B / S07-60C	
	$\Delta M_i/M^O$	$\Delta M_i/M_i^O$	$\Delta M_i/M^O$	$\Delta M_i/M_i^O$	$\Delta M_i/M^O$	$\Delta M_i/M_i^O$	$\Delta M_i/M^O$	$\Delta M_i/M_i^O$
SiO_2	−13.1	−0.19	−9.58	−0.16	−27.2	−0.45	0.00	0.00
TiO_2	0.07	0.34	−0.15	−0.50	1.83	6.09	−0.30	−1.00
Al_2O_3	0.00	0.00	−14.4	−0.92	−7.48	−0.48	1.62	0.10
Fe_2O_3	1.38	2.41	0.68	0.33	1.54	0.74	−1.63	−0.79
FeO	0.30	0.24	1.75	1.07	2.08	1.27	−1.00	−0.61
FeO_{tot}	1.54	0.88	2.36	0.68	2.36	0.67	−2.47	−0.71
MnO	0.07	2.45	0.32	2.89	0.08	0.68	−0.08	−0.74
MgO	0.71	1.61	1.72	1.41	0.69	0.56	−0.86	−0.70
CaO	2.25	1.01	35.0	7.34	36.4	7.63	−3.04	−0.64
Na_2O	1.16	0.19	−6.61	−0.84	−4.50	−0.57	0.68	0.09
K_2O	0.21	0.09	−2.60	−0.96	−2.04	−0.75	−0.27	−0.10
P_2O_5	0.18	2.29	2.18	7.79	1.36	4.86	−0.21	−0.76
$C(CO_2)$	0.67	–	3.58	5.04	13.2	18.6	−0.71	−1.00
Cl	−0.001	−0.06	0.01	1.44	0.009	1.05	0.00	−0.05
F	−0.01	−0.26	0.16	5.38	0.13	4.58	−0.02	−0.74
Ba	604	0.77	−1379	−0.93	−704	−0.48	−481	−0.33
Sr	668	1.20	492	0.38	14100	10.8	−680	−0.52
Li	−4.71	−0.54	−1.95	−0.45	0.57	0.13	−3.35	−0.77
Rb	−28.8	−0.54	−24.4	−0.94	−12.7	−0.49	−7.84	−0.30
Cs	−0.15	−0.59	0.07	0.63	0.14	1.31	0.03	0.31
Zr	67.0	1.11	−52.2	−0.39	70.4	0.52	−116	−0.86
Hf	0.86	0.48	−1.19	−0.42	2.54	0.90	−2.19	−0.78
Ta	0.58	0.08	−3.87	−0.49	85.5	10.7	0.31	0.04
Nb	33.7	0.53	61.8	0.60	359	3.47	−76.4	−0.74
Y	0.85	0.20	24.0	4.42	31.8	5.84	−3.93	−0.72
Sc	−33.7	−0.77	−1.69	−0.15	−2.97	−0.27	8.20	0.75
La	16.1	0.59	173	3.73	592	12.8	−24.7	−0.53
Ce	25.5	0.43	276	3.06	839	9.31	−57.5	−0.64
Pr	3.60	0.62	24.6	2.46	76.8	7.68	−7.03	−0.70
Nd	10.6	0.63	62.6	2.14	219	7.51	−21.0	−0.72
Sm	2.20	0.72	10.7	1.92	22.2	3.99	−4.22	−0.76
Eu	0.65	0.77	2.64	1.67	6.16	3.89	−1.11	−0.70
Gd	1.74	0.65	11.6	2.48	27.4	5.83	−3.57	−0.76
Tb	0.15	0.70	0.95	2.47	2.43	6.32	−0.30	−0.78
Dy	0.62	0.64	5.42	3.22	7.87	4.67	−1.34	−0.80
Ho	0.09	0.55	0.93	3.31	0.97	3.46	−0.22	−0.79
Er	0.32	0.83	2.43	3.18	2.62	3.43	−0.60	−0.78
Tm	0.05	1.11	0.31	3.32	0.32	3.43	−0.07	−0.75
Yb	0.38	1.58	1.89	2.87	1.71	2.60	−0.52	−0.79
Lu	0.06	1.82	0.31	3.55	0.14	1.63	−0.07	−0.75
MC	−6.03		15.61		15.53		−5.05	
VC	−1.76		–		–		−2.57	
IP	Al_2O_3 FeO K_2O		V = const		V = const		SiO_2 K_2O	

$\Delta M_i/M_0$ is the mass balance relative to the protolith mass (g/100 g for oxides and mg/1000 g for elements); $\Delta M_i/M_i^O$ is the mass balance relative to the mass of the element in the protolith, MC is the change of protolith mass in % (gain + loss), VC is the change of protolith volume in % (gain + loss), IP is an inert component, and V = const denotes the estimation of gain and loss assuming constant volume.

* Composition of protolith.

** Composition of the products of metasomatic alteration. Samples: S07-60A is fenitized gneiss, S07-60B is fenite, S07-60C is albitite, S07-60F is wollastonite–clinopyroxene rock, and 2048/263.3 is carbonated silicate rock of the K-feldspar–calcite temperature facies.

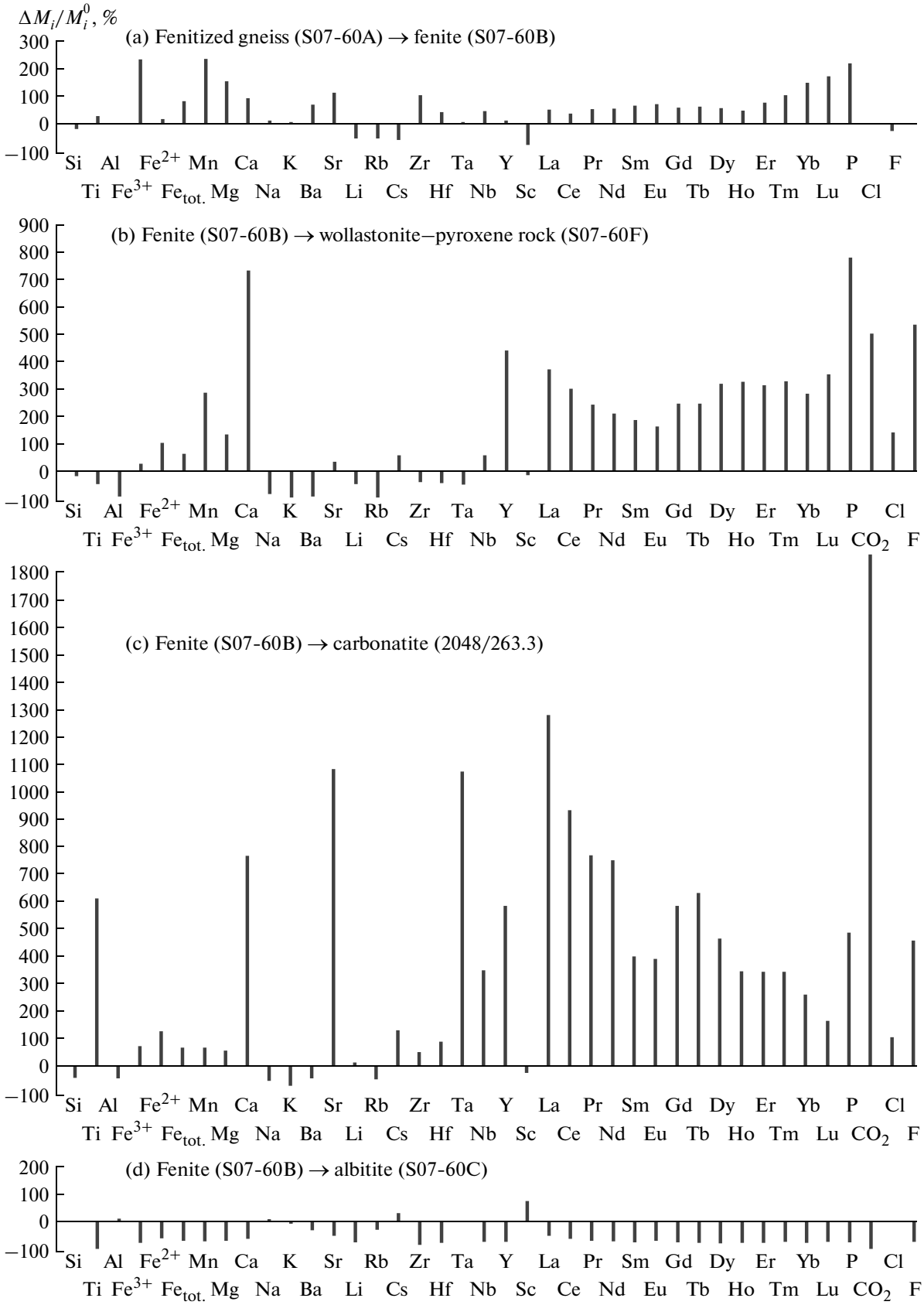

Fig. 4. Histograms of changes in the masses of components ($\Delta M_i/M_i^O$) relative to their masses in the protolith (in %) for different rock pairs.

Table 9. Isotopic composition and content of He trapped in fluid inclusions and contents of U, Th, and Li in crushed mineral separates of aegirine–augite (*Aeg–Aug*$_1$) and wollastonite (*Wo*) and whole-rock carbonatite sample OV-18

Sample	^{4}He, 10^{-6} cm^3/g	^{3}He/^{4}He, 10^{-8}	He$_m$, %	U, ppm	Th, ppm	Li, ppm
Aeg-Aug$_1$	10.0–10.9	591–594	49	0.2	14.4	4.3
Wo	0.42–0.96	45–52	3–4	0.1	0.99	0.6
OV-18*	0.29	105	9	–	–	–

The maximum measured values are given for U, Th, and Li contents.

* After Tolstikhin et al. (1999).

groups of REE: $\Delta M_i/M_i^O$ is 190–370% for most of the elements, except for Y (440%) and Eu (170%). The modeling of metasomatic transformation of the fenite after gneiss to the carbonatite of the K-feldspar–calcite temperature facies suggests a systematic increase in the degree of REE enrichment from HREE ($\Delta M_i/M_i^O$ = 160% for Lu) to LREE ($\Delta M_i/M_i^O$ = 1280% for La). The behavior of HFSE is variable. During the formation of the wollastonite–clinopyroxene rocks, they are removed from the fenites (Zr, Hf, and Ta) or show low mobility (Nb), whereas the formation of the carbonatites was accompanied by the accumulation of all HFSE, especially Nb and Ta. Both models indicated significant relative enrichment in all volatile components: $\Delta M_i/M_i^O$ is 490–780% for P_2O_5, 500–1860% for CO_2, 100–140% for Cl, and 460–540% for F. The calculations showed that the fenite-to-albitite transformation requires the removal of most major and trace components (Fig. 4d). The only exceptions among the trace elements are Sc, which was accumulated in the albitites, and Ta and Cs, which showed only minor variations.

HELIUM ISOTOPE SYSTEMATICS IN THE CONTACT ROCKS

In order to estimate the degree of contamination of solutions by crustal materials at various stages of the metasomatic process, we investigated the isotopic composition of He captured in fluid inclusions during crystallization. Monomineralic fractions of aegirine–augite of the early alkaline assemblage and wollastonite were used as initial materials for He analysis. Gas from these mineral samples was released by crushing under vacuum. Such a method of sample destruction results in gas extraction from gas–liquid inclusions, whereas most of the radiogenic He accumulated in minerals during their history remains in the crushed material. In the materials remained after analysis, we determined the contents of the main ^{4}He-producing elements, U and Th, as well as Li (^{3}He is formed from ^{6}Li in nuclear reactions), which appeared to be very low. The contribution of radiogenic He could not significantly disturb the primary isotopic composition of the trapped gas. The measured isotopic compositions and contents of He are shown in Table 9. The fraction of mantle He (He$_m$) was estimated using the equation

$$\mathrm{He}_m(\%) = \frac{(^3\mathrm{He}/^4\mathrm{He}_{\mathrm{meas}} - ^3\mathrm{He}/^4\mathrm{He}_{\mathrm{crust}})}{^3\mathrm{He}/^4\mathrm{He}_{\mathrm{mantle}}} \times 100,$$

at ^{3}He/^{4}He$_{crust}$ = (0.5–5.0) × 10^{-8} and ^{3}He/^{4}He$_{mantle}$ = 1.2 × 10^{-5} (Prasolov, 1990). For comparison, also shown is the isotopic composition of He from carbonatite drill core sample OV-18 (Tolstikhin et al., 1999) collected within the southwestern contact aureole of the intrusion, 100 m below our cross-section. Helium contents and isotope ratios in the gases of fluid inclusions from the carbonatite and wollastonite samples are similar. In both cases, He$_m$ is no higher than 10%, which suggests a high degree of crustal contamination. The obtained ^{3}He/^{4}He values for clinopyroxene are an order of magnitude higher than those for wollastonite samples. The value He$_m$ = 49% indicates a significant contribution of the mantle component.

DISCUSSION

Stages and Conditions of Metasomatic Alteration

The amounts of olivinites and pyroxenites in the Ozernaya Varaka Massif are minor, and no metasomatic products of gneiss interaction with these rocks were found in the cross-sections and drill core samples examined by us. The wide aureole of high-temperature comagmatic alkaline metasomatic rocks surrounding the massif (fenitized gneisses and fenites) was produced by the injection of foidolite magmas through ring faults. During this stage, the minerals of the early alkaline assemblage were formed and replaced protolith minerals. The subsequent intrusion of carbonatite magmas also affected the previously formed rocks of the foidolite series of the massif and the surrounding gneisses. This is identified from changes in the petrochemical characteristics of the rocks and appearance of the minerals of the basic assemblage, which were detected in almost all of our samples. This fact indicates the importance of the carbonatite process for the development of the present-day appearance of rocks in the fenitization zone, despite the local occurrence of the carbonatite complex in the fenite aureole. The similarity (within the massif) of the structural positions and formation

mechanisms of the wollastonite–pyroxene rocks and the highest temperature carbonatites of the K-feldspar–calcite facies, their mineralogical and geochemical features, and the similarity of He isotope characteristics suggest a genetic relation between the high-temperature basic metasomatism in the contact aureole and the carbonatite process. The rocks were affected both in the contact aureole and in the border zone of the intrusion. The latter were transformed to magnesian pyroxenites after ijolites similar to the wollastonite–clinopyroxene rocks in terms of both major- and trace-element geochemistry. The latest metasomatic processes occurred at the postmagmatic stage and produced a complex of late alkaline metasomatites (albitites, K-feldspar metasomatic rocks, glimmerites, etc.). Their relation to the retrograde stage of the carbonatite process cannot be ruled out; our model calculations showed that this stage was accompanied by the removal of the same components that were accumulated during albitization (Al, Na, and Si). This suggestion is indirectly supported by the frequently observed overlapping of the products of high-temperature basification and late alkaline metasomatism, as well as the presence of a feldspar zone at the metasomatic replacement front around the veins of carbonated silicate rocks of the K-feldspar–calcite facies.

Composition and Mechanisms of Migration of Metasomatizing Solutions

Variations in the anion composition of the fluid phase at different stages of metasomatic alteration were estimated using the calculated gain and loss values for volatiles during the formation of various types of metasomatic rocks, which provided indirect evidence for changes in the activities (and, correspondingly, concentrations) of fluid components (Table 8). The following is a possible general scenario for the evolution of metasomatizing solutions.

High-temperature alkaline metasomatism occurred under the influence of a water-dominated fluid phase poor in other volatile components. This is consistent with the existing concepts on the composition of solutions released from an "ijolite" source (*Metasomatism ...,* 1998). The great thickness of the fenitization aureole indicates that a considerable volume of fluid reacted with the country rocks during this stage. Our investigations suggest that the solution was separated directly from a magma reservoir, which is the reason for the high fraction of mantle He. The persistent compositions of minerals of the early alkaline assemblage, which was formed at this stage, through the whole fenite zone suggest the dominance of infiltration mass transfer during the formation of the proximal zone of the fenitization column. The neutral water–carbon dioxide fluid that caused **basic metasomatism** in the contact zone was transported along a system of fractures and shatter zones from the root of the magmatic system, which is reflected in the crustal contamination of the composition of noble gases. The fluid phase was characterized by a complex anion composition with high concentrations of F, Cl, P, and S. The interaction of the infiltrating solution with the fenites and ijolites adjoining the zone of wollastonite–clinopyroxene rocks was mainly diffusion-controlled, which is suggested by the wide variations of the compositions of minerals formed during this stage even in a single sample. The petrochemical characteristics of zone III rocks and mass balance calculations suggest that the **albitites** were formed under the influence of an aqueous fluid with low contents of other volatile components. The infiltration character of mass transfer is supported by the stable compositions of minerals (feldspars and apatite) that crystallized during this stage. The presence of albitized rocks not only in the fenites of the contact aureole but also within the intrusion is explained by the formation of fluid-permeable fracture systems after the crystallization of rocks in the massif.

Behavior of Major and Trace Elements during Various Stages of Metasomatic Alteration

During the **fenitization** stage, alkali and alkali earth elements were intensely transported from the intrusion into the aluminosilicate country rocks. The formation of the proximal zone of the metasomatic column was accompanied by the release of SiO_2 from the gneisses, which was partly immobilized at the front of the fenite zone. Despite the intensity of contact metasomatism, only moderate accumulation of HFSE and REE was observed, which was probably related to their low mobility in a fluid poor in halogens, P, and S. Our model calculations showed that the behavior of geochemically similar HFSE (Zr and Hf or Nb and Ta) was different during early alkaline metasomatism. In particular, Zr was most likely more mobile than Hf, and, despite the significant relative enrichment of fenites in Nb, there was no significant Ta accumulation. The accumulation of REE was also selective with a tendency of enrichment in the heavy REE.

During **high-temperature basic metasomatism**, all components were perfectly mobile. The almost complete removal of alkalis and Al and significant Si loss were accompanied by the extensive accumulation of bases, primarily Ca. Owing to the entrainment of material from the root zone of the magmatic system, solutions were derived from a "carbonatitic" source, which probably resulted in a sharp increase in the contents of F and other volatile components (CO_2, P, and S) in the fluid system. The combined effect of two factors, an REE-rich source and hydrothermal solution with efficient extracting properties, resulted in REE input into the contact zone. The HFSE enrichment established in the carbonatites of the K-feldspar–calcite facies and the low contents of these elements in the wollastonite–clinopyroxene metasomatic rocks and carbonatites of the albite–calcite temperature facies

(Tables 5, 6) indicate that HFSE were immobilized in the earliest high-temperature products of basic metasomatism, which resulted in the deficiency of these elements in residual fluids. The formation of **albitites** was accompanied by the gain of Al and Na and loss of Ca, Mg, Fe^{2+}, and Fe^{3+}. Based on the calculation of the numbers of atoms in the reference volume (1000 Å) for various types of rocks from the contact aureole (Table 7), it was shown that the formation of the high-temperature basic metasomatic rocks (carbonatites of the K-feldspar–calcite temperature facies and wollastonite–clinopyroxene rocks) resulted in the removal from the reference volume of fenites after gneisses of 4.6–10.5 Si atoms, 2.2–4.3 Al atoms, and 1.6–2.6 Na atoms, whereas the formation of albitites from the fenites after gneisses involved the input of 2.0 Si atoms, 1.0 Al atom, and 1.4 Na atoms. It can be calculated that the amount of material extracted into the fluid phase during the formation of the basic metasomatites is sufficient to produce albitite in the proportion 2–4 volumes of albitite per one volume of basic metasomatic rock. The divalent bases and Fe^{3+} removed during albitization and the excess K and Na generated owing to the formation of basic metasomatic rocks were probably immobilized in phlogopite glimmerites and aegirinites, which were documented within the contact aureole. Our modeling showed that the albitization process was accompanied by the removal of almost all of the trace elements analyzed, except for Sc, Ta, and Cs. Noteworthy is the fractionation of geochemically similar HFSE, primarily, Nb and Ta, during the early (fenitization) and late (albitization) stages of alkaline metasomatism (Table 8). The source of matter during fenite formation was the HFSE-rich foidolites; therefore, the solution was relatively rich in most HFSE, but not Ta, which is suggested by the calculations. This fact can be interpreted in terms of acid–base interaction, which implies that alkaline fluid extracts more efficiently more acidic components; this was the reason for the low mobility of Ta, as a stronger base. For the same reason, Ta was not extracted from previously formed rocks during albitization under the influence of a fluid probably poor in HFSE, because of its higher relative activity, which explains the maximum Ta/Nb values observed in the albitites. A similar interpretation can be proposed for the fractionation of LREE and HREE, which also show different acid–base properties. Since the Y-group REE are more acidic components, they must be more efficiently extracted by alkaline fluids, which resulted in the selective accumulation of REE and relative HREE enrichment observed in the fenites.

Differences between the Contact Reaction Zones of Agpaitic Syenites and Alkaline Ultrabasic Complexes

A comparison of our results with data on the contact reaction zones of the Khibiny and Lovozero agpaitic massifs (Arzamastsev et al., 2011) revealed a number of significant differences.

(1) Disparity in the relative size of fenite aureoles. The contact reaction zones at the giant massifs of Khibiny and Lovozero are a few tens of meters wide, whereas similar zones around alkaline ultrabasic complexes are comparable in size with the intrusions themselves.

(2) The fluids of the contact zones of alkaline ultrabasic massifs are H_2O- and CO_2-dominated, whereas the rocks of the contact aureoles of agpaitic massifs are enriched in F. The fenitized rocks of the Lovozero massif contain fluorite, and their F content is up to 0.58–0.70 wt %.

(3) The degrees of HFSE and REE mobility in the processes of contact interaction of alkaline ultrabasic and agpaitic magmas with the enclosing gneisses are different. Mass balance calculations showed that, at similar concentrations of these components in the protoliths, the absolute gain and loss values ($\Delta M_i / M^O$) for the models of fenite formation at agpaitic complexes are 3–10 times higher than those for the fenites of the Ozernaya Varaka alkaline ultrabasic massif.

A possible explanation for the nature of these observations is the different compositions of fenitization agents for the alkaline ultrabasic and agpaitic syenite complexes. Decompression degassing accompanying the emplacement of alkaline magmas produced a considerable volume of a fluid phase from the earliest stages of the development of alkaline complexes (Kogarko and Ryabchikov, 1978). On the other hand, the solubility of water and other volatile components depends significantly on the chemical composition of melt and increases with increasing alkalinity (Kogarko, 1977). Because of this, the solubility of water in alkaline ultrabasic melts is significantly lower than in agpaitic melts. As a result, the fenitizing solution of alkaline ultrabasic complexes was released at a higher temperature stage into the country rocks whose fluid permeability increased owing to thermal decompaction. Since the fluid–alkaline melt partition coefficient of F (K_D) is much lower than one (Kogarko and Krigman, 1981), the fenitizing solution of alkaline ultrabasic complexes was depleted in this element together with other volatile components (CO_2, Cl, and S). It was shown that the presence of F controls to a large extent the migration of such weakly mobile components as HFSE and REE (Rubin et al., 1993; Gramenitskii et al., 2005); this effect may account for the low input of HFSE and REE during the formation of fenites at alkaline ultrabasic complexes. The release of metasomatizing fluid accompanying the development of agpaitic plutons occurred differently. The small scale of country rock alteration is probably related to the high water solubility in agpaitic melts, which prevented the separation of a vapor–gas phase. Moreover, the crystallization of hydrous agpaitic magmas may result in a transition from silicate melt to residual

brine, which can efficiently extract REE (Kogarko, 1977; Gramenitskii et al., 2005). Perhaps, the fenite aureoles of the Khibiny and Lovozero massifs were formed at late magmatic stages of their evolution under the influence of a heterogeneous fluid consisting of aqueous hydrothermal solution and high-density fluoride brine. This suggestion is supported by the dating of zircon from the zone of contact metasomatic rocks of the Lovozero massif, which showed that they were formed several million years after the main stage of agpaitic syenite development (Arzamastsev et al., 2007). The generation of a fluid phase occurred in a narrow border zone up to 200 m wide, rather than in the whole volume of the magma chamber. The release of fluid modified the composition of rocks in this zone, which are strongly different from the nepheline syenites in the interior of the massif.

CONCLUSIONS

The investigations reported here allowed us to distinguish factors controlling the formation of various types of hydrothermal–metasomatic rocks in the contact aureole of the Ozernaya Varaka alkaline ultrabasic complex and their geochemical signatures. The results can be summarized as follows.

(1) The contact aureole bears evidence for the activity of a long-lived metasomatic system, which underwent convergent modifications manifested by the change of source materials. It was related to the sequential intrusion of alkaline silicate and carbonatite melts, chemical evolution of the fluid phase, and change in the mechanisms of solution migration, which is reflected in regular variations in geological, petrographic, mineralogical, geochemical, and isotopic characteristics of contact metasomatic rocks of different age.

(2) Model calculations showed that, despite the extensive contact metasomatic alteration accompanying the formation of foidolite rocks, the transport of trace elements into the country rocks was insignificant. The observed enrichment of the rocks of the contact aureole in REE was caused by superimposed high-temperature basic metasomatism, which was probably related to the entrainment of material from a carbonatite source and the specific anion composition of the fluid phase.

(3) A comparison of the contact zones of the Ozernaya Varaka alkaline ultrabasic–carbonatite complex and the Khibiny and Lovozero agpaitic syenite massifs revealed significant mineralogical and geochemical differences, which can be interpreted as resulting from the different compositions of fenitizing agents and amounts of released fluids. Tremendous volumes of aqueous solutions poor in other volatile components infiltrated into the country rocks during the formation of the fenite aureoles of alkaline ultrabasic complexes. The metasomatic alteration of gneisses enclosing the agpaitic syenite plutons was caused by minor volumes of heterogeneous fluids consisting of a hydrothermal aqueous solution and a high-density fluoride brine.

ACKNOWLEDGMENTS

Helium isotope compositions and contents were determined in our samples in collaboration with I.L. Kamensky and V.I. Skiba (Geological Institute, Kola Science Center, Russian Academy of Sciences). The electron microscope investigation of mineral phases was carried out by A.V. Bazai (Geological Institute, Kola Science Center, Russian Academy of Sciences). The ICP-MS analysis of trace elements was conducted by I.R. Elizarova (Tananaev Institute of Chemistry and Technology of Rare Elements and Mineral Raw Materials, Kola Science Center, Russian Academy of Sciences). We thank I.T. Rass (Institute of Geology of Ore Deposits, Petrography, Mineralogy, and Geochemistry, Russian Academy of Sciences) for a constructive and friendly review.

This study was financially supported by the Russian Foundation for Basic Research, project no. 12-05-00244.

REFERENCES

Anders, E. and Grevesse, N., Abundances of the elements: meteoritic and solar, *Geochim. Cosmochim. Acta*, 1989, vol. 53, pp. 197–214.

Andersen, T., Carbonatite-related contact metasomatism in the Fen complex, Norway: effects and petrogenetic implications, *Mineral. Mag.*, 1989, vol. 53, pp. 395–414.

Arzamastsev, A.A., Bea, F., Glaznev, V.N., et al., Kola alkaline province in the Paleozoic: estimation of composition of primary mantle melts and conditions of magma generation, *Ross. Zh. Nauk Zemle*, 2001, vol. 3, no. 1, pp. 3–24.

Arzamastsev, A.A., Arzamastseva, L.V., Travin, A.V., et al., Duration of formation of magmatic system of polyphase Paleozoic alkaline complexes of the Central Kola: U–Pb, Rb–Sr, Ar–Ar Data, *Dokl. Earth Sci.*, 2007, vol. 413, no. 5, pp. 666–670.

Arzamastsev, A.A., Fedotov, Zh.A., and Arzamastseva, L.V., *Daikovyi magmatizm severo-vostochnoi chasti Baltiiskogo shchita* (Dike Magmatism of the Northeastern Baltic Shield), St. Petersburg: Nauka, 2009.

Arzamastsev, A.A., Arzamastseva, L.V., and Zaraisky, G.P., Contact interaction of agpaitic magmas with basement gneisses: an example of the Khibina and Lovozero massifs, *Petrology*, 2011, vol. 19, no. 2, pp. 109–133.

Bardina, N.Yu. and Popov, V.S., Fenites: systematic, conditions of formation, and significance for crustal magma formation, *Zap. Vseross. Mineral. O-va*, 1994, vol. 133, no. 6, pp. 1–19.

Cawthorn, K.D. and Collerson, K.D., The recalculation of pyroxene end-member parameters and the estimation of ferrous and ferric iron content from electron microprobe analyses, *Am. Mineral.,* 1974, vol. 59, pp. 1203–1208.

Coelho, J., GEOISO—a Windows(tm) program to calculate and plot the mass balances and the volume changes

occurred in a wide variety of geologic processes, *Comp. Geosci.*, 2006, vol. 32, no. 9, pp. 1523–1528.

Currie, K.L. and Ferguson, J., A study of fenitization around the alkaline carbonatite complex at Callander Bay, Ontario, Canada, *Can. J. Earth Sci.*, 1971, vol. 8, pp. 498–518.

Drüppel, K., Hoefs, J., and Okrusch, M., Fenitizing processes induced by ferrocarbonatite magmatism at Swartbooisdrif, NW Namibia, *J. Petrol.,* 2005, vol. 46, no. 2, pp. 377–406.

Dudkin, O.B., Savitskii, A.V., and Kuleshov, G.V., Mineral associations of the alkaline complex of the Ozernaya Varaka massif, in *Mineral'nye kompleksy i mineraly Kol'skogo poluostrova* (Mineral Complexes and Minerals of the Kola Peninsula), Apatity: Izd-vo KFAN RAN SSSR, 1980, pp. 126–140.

Evdokimov, M.D., *Fenity Tur'inskogo shchelochnogo kompleksa Kol'skogo poluostrova (mineral'nye assotsiatsii i geokhimicheskie osobennosti)* (Fenites of the Turyi Alkaline Complex of the Kola Peninsula (Mineral Assemblages and Geochemical Features)), Leningrad: Izd-vo Leningradskogo universiteta, 1982.

Glossary of Geology, Gary, M., McAfee, R.Jr., and Wolf, C.L., Eds., Washington, DC: American Geological Institute, 1974.

Gramenitskii, E.N., Shchekina, T.I., and Devyatova, V.N., *Fazovye otnosheniya vo ftorsoderzhashchei granitnoi i nefelin-sienitovoi sistemakh i raspredelenie elementov mezhdu fazami (eksperimental'noe issledovanie)* (Phase Relations in Flluorine-Bearing Granite and Nepheline-Syenite Systems and Partition of Elements between Phases), Moscow: GEOS, 2005.

Grant, J.A., The isocon diagram—a simple solution to Gresens' equation for metasomatic alteration, *Econ. Geol.*, 1986, vol. 81, no. 8, pp. 1976–1982.

Gresens, R.L., Composition–volume relationships of metasomatism, *Chem. Geol.*, 1967, vol. 2, no. 1, pp. 47–55.

Kazitsyn, Yu.K. and Rudnik, V.A., *Rukovodstvo k raschetu balansa veshchestva i vnutrennei energii pri formirovanii metasomaticheskikh porod* (Guide to the Calculation of Mass-Balance and Internal Energy during Formation of Metasomatic Rocks), Moscow: Nedra, 1968.

Kogarko, L.N., *Problemy genezisa agpaitovykh magm* (Genesis of Peralkaline Magmas), Moscow: Nauka, 1977.

Kogarko, L.N. and Krigman, L.D., *Ftor v silikatnykh rasplavakh i magmakh* (Fluorine in Silicate Melts and Magmas), Moscow: Nauka, 1981.

Kogarko, L.N. and Ryabchikov, I.D., Volatiles in magmatic processes, *Geokhimiya*, 1978, no. 9, pp. 1293–1321.

Kramm, U., Kogarko, L.N., Kononova, V.A., and Vartiainen, H., The Kola alkaline province of the CIS and Finland: precise Rb–Sr ages define 380–360 age range for all magmatism, *Lithos*, 1993, vol. 30, pp. 33–44.

Kresten, P. and Morogan, V., Fenitization at the Fen complex, southern Norway, *Lithos,* 1986, vol. 19, pp. 27–42.

Kukharenko, A.A., Orlova, M.P., Bulakh, A.G., et al., *Kaledonskii kompleks ul'traosnovnykh, shchelochnykh porod i karbonatitov Kol'skogo poluostrova i Severnoi Karelii* (Caledonian Complex of Ultrabasic and Alkaline Rocks and Carbonatites of the Kola Peninsula and North Karelia), Moscow: Nedra, 1965.

Leake, B.E., Woolley, A.R., Arps, C.E.S., et al., Nomenclature of amphiboles: report of the Subcommittee on Amphiboles of the International Mineralogical Association, Commission on New Minerals and Mineral Names, *Can. Mineral.*, 1997, vol. 35, pp. 219–246.

Metasomatizm i metasomaticheskie porody (Metasomatism and Metasomatic Rocks), Zharikov, V.A., Rusinov, V.L., Eds., Moscow: Nauchnyi mir, 1998.

Morimoto, N., Nomenclature of pyroxenes, *Can. Mineral.*, 1989, vol. 27, pp. 143–156.

Morogan, V., Ijolite versus carbonatite as sources of fenitization, *Terra Nova*, 1994, vol. 6, no. 2, pp. 166–176.

Prasolov, E.M., *Izotopnaya geokhimiya i proiskhozhdenie prirodnykh gazov* (Isotope Geochemistry and Origin of Natural Gases), Leningrad: Nedra, 1990.

Rass, I.T., Abramov, S.S., Utenkov, V.A., et al., Role of fluid in the genesis of carbonatites and alkaline rocks: geochemical evidence, *Geochem. Int.*, 2006, vol. 44, no. 7, pp. 636–655.

Rizvanova, N.G., Levchenkov, O.A., Bogomolov, E.S., et al., Comparison of zircon separation techniques for geochronological purposes, *Geokhimiya,* 1994, no. 7, pp. 1076–1087.

Rubie, D.C. and Gunter, W.D., The role of speciation in alkaline igneous fluids during fenite metasomatism, *Contrib. Mineral. Petrol.*, 1983, vol. 82, pp. 165–175.

Rubin, J.N., Henry, C.D., and Price, J.G., The mobility of zirconium and other "immobile" elements during hydrothermal alteration, *Chem. Geol.*, 1993, vol. 110, pp. 29–47.

Rudnick, R.L. and Gao, S., The composition of the continental crust, in *The Crust. Treatise on Geochemistry*, Holland, H.K. and Turekian, K.K., Eds., Oxford: Elsevier-Pergamon, 2003, vol. 3, pp. 1–64.

Samoilov, V.S., *Geokhimiya karbonatitov* (Geochemistry of Carbonatites), Moscow: Nauka, 1984.

Sergeev, A.S., Fenites and fenitization in the contact aureole of the alkaline and ultrabasic intrusions of the Khabozero Group (Kola Peninsula), *Zap. Vseross. Mineral. O-va*, 1959, vol. 88, no. 4, pp. 430–443.

Sindern, S. and Kramm, U., Volume characteristics and element transfer of fenite aureoles: a case study from the Iivaara alkaline complex, Finland, *Lithos*, 2000, vol. 51, pp. 75–93.

Sokolov, S.V., Formation temperatures and temperature facies of carbonatites from the alkaline ultramafic complexes, *Geochem. Int.,* 1996, no. 1, pp. 13–18.

Taylor, S.R. and McLennan, S.M., The geochemical evolution of the continental crust, *Rev. Geophys.*, 1995, vol. 33, pp. 241–265.

Tolstikhin, I.N., Kamensky, I.L., Marty, B., et al., Identification of the low mantle plume substance in the Devonian alkaline–ultrabasic–carbonatite complexes of the Kola Peninsula on the basis of the study of noble gas and radioactive element isotopes, *Preprint*, KNTs RAN: Apatity, 1999.

Wedepohl, K.H., The composition of the continental crust, *Geochim. Cosmochim. Acta*, 1995, vol. 59, pp. 1217–1232.

Translated by A. Girnis